FEDERAL UNIVERSITY OF PARÁ

INSTITUTE OF TECHNOLOGY

GRADUATE PROGRAM IN ELECTRICAL ENGINEERING

# A COMPARISON OF DIMENSIONALITY REDUCTION AND BLIND SOURCE SEPARATION TECHNIQUES FOR VIDEO-BASED MODAL IDENTIFICATION

## THAISSE DIAS PAES

UFPA / ITEC / PPGEE

Guamá University Campus
Belém-Pará-Brazil

2023

FEDERAL UNIVERSITY OF PARÁ

INSTITUTE OF TECHNOLOGY

GRADUATE PROGRAM IN ELECTRICAL ENGINEERING

DM: 12/23

THAISSE DIAS PAES

# A COMPARISON OF DIMENSIONALITY REDUCTION AND BLIND SOURCE SEPARATION TECHNIQUES FOR VIDEO-BASED MODAL IDENTIFICATION

UFPA / ITEC / PPGEE

Guamá University Campus
Belém-Pará-Brazil

2023

FEDERAL UNIVERSITY OF PARÁ

INSTITUTE OF TECHNOLOGY

GRADUATE PROGRAM IN ELECTRICAL ENGINEERING

THAISSE DIAS PAES

# A COMPARISON OF DIMENSIONALITY REDUCTION AND BLIND SOURCE SEPARATION TECHNIQUES FOR VIDEO-BASED MODAL IDENTIFICATION

Masters dissertation submitted to the Examining Board of the Graduate Program in Electrical Engineering from the Federal University of Pará as partial requirement to obtain the Master's Degree in Electrical Engineering, Area of Concentration in Signal Processing.

UFPA / ITEC / PPGEE

Guamá University Campus
Belém-Pará-Brazil

2023

UNIVERSIDADE FEDERAL DO PARÁ
INSTITUTO DE TECNOLOGIA
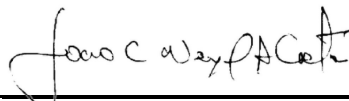PROGRAMA DE PÓS-GRADUAÇÃO EM ENGENHARIA ELÉTRICA

**"A COMPARISON OF DIMENSIONALITY REDUCTION AND BLIND SOURCE SEPARATION TECHNIQUES FOR VIDEO-BASED MODAL IDENTIFICATION"**

AUTORA: **THAISSE DIAS PAES**
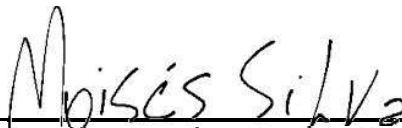
DISSERTAÇÃO DE MESTRADO SUBMETIDA À BANCA EXAMINADORA APROVADA PELO COLEGIADO DO PROGRAMA DE PÓS-GRADUAÇÃO EM ENGENHARIA ELÉTRICA, SENDO JULGADA ADEQUADA PARA A OBTENÇÃO DO GRAU DE MESTRA EM ENGENHARIA ELÉTRICA NA ÁREA DE TELECOMUNICAÇÕES.

APROVADA EM: 29/03/2023

**BANCA EXAMINADORA:**
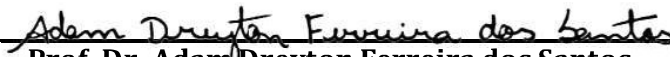
_____
**Prof. Dr. João Crisóstomo Weyl Albuquerque Costa**
(Orientador – PPGEE/UFPA)

_____
**Prof. Dr. Moisés Felipe Mello da Silva**
(Coorientador – POSTDOCTORAL RESEARCH ASSOCIATE/LOS ALAMOS NATIONAL LABORATORY)

_____
**Prof.ª Dr.ª Jasmine Priscyla Leite de Araújo**
(Avaliadora Interna – PPGEE/UFPA)

_____
**Prof. Dr. Adam Dreyton Ferreira dos Santos**
(Avaliador Externo – UNIFESSPA)

**VISTO**:

_____
**Prof. Dr. Diego Lisboa Cardoso**
(Coordenador do PPGEE/ITEC/UFPA)

*À doce memória de meu avós:*
*Vanderlina da Silva Paes e João Paes Cardias;*
*Manoel Souza Dias e Osmarina Araujo Dias.*

*"Não tenho mais saudade dos tristes caminhos por onde passei.*
*Pois a felicidade que eu almejava, agora encontrei."*

# Acknowledgements

Ao Dr. Moisés Felipe Mello da Silva agradeço pela coorientação, pelo tema sugerido, pela paciência e persistência. Muito obrigada por tudo.

Gostaria de expressar minha gratidão ao Professor João Crisóstomo Weyl Albuquerque Costa pela orientação a confiança neste trabalho.

A Juan Vidal agradeço pela amizade e suporte. Sua presença em minha vida permanece sendo um dos grandes presentes que recebi da vida acadêmica.

Eu sou privilegiada por ter nascido na melhor família possível. Meus agradecimentos à Jacilene Araújo Dias, Abdene da Silva Paes, Leonardo Araújo Dias Paes e Levy Araújo Dias Paes. Obrigada pela proteção e pelo amor diário.

Ao meu irmão João Thiago Dias Paes, pela torcida e companheirismo. Você é meu exemplo de amor pelo trabalho e determinação em realizá-lo da melhor maneira possível.

Aos meus pais Mizack da Silva Paes e Janete Dias Paes, meus amores. Obrigada pelo dom da vida, pelo incentivo e confiança. Nada seria possível sem vocês. A vocês todo meu amor, respeito e gratidão.

*"Wir müssen wissen.*
*Wir werden wissen."*

*"We must know.*
*We shall know."*
The epitaph on David Hilbert gravestone.

# Abstract

Understading the dynamic properties of a structural system is indispensable for a reliable study of the structural behavior. Video-based structural dynamics identification has been effectively used as a key method for modal analysis in recent years. With several different approaches, the ones based on the blind source separation strategy have received increased attention for identifying structural characteristics. Blind source separation addresses the problem of separating or extracting the original source waveforms from a sensor array. Although the literature addresses several techniques to perform the source separation, only one of them (named complexity pursuit) is often employed for video-based solutions. This work aims to explore other blind source separation algorithms to perform video-based modal analysis. In order to perform the modal decomposition, a set of blind source separation methods is combined with different dimensionality reduction techniques for full-field high-resolution structural dynamics from video. Specifically, Principal Component Analysis (PCA) and Nonnegative Matrix Factorization (NNMF), two dimensionality reduction techniques, are used for video compression along with six source separation algorithms, resulting in twelve different frameworks tested over a laboratory cantilever beam structure and a bench-scale model of a three-story building structure. The blind source separation techniques used are: Complexity Pursuit (CP), Idependent Component Analysis (ICA), Second Order Blind Identification (SOBI), Second Order Blind Identification with Robust Orthogonalization (SOBIRO), Equivariant Robust Idependent Component Analysis (ERICA) and Algorithm for Multiple Unknown Signals Extraction (AMUSE). The twelve techniques based on dimensionality reduction and blind source separation algorithms are evaluated here using as the criteria comparison their mode shape, modal coordinates and MAC values. The main goal is to provide a range of alternatives for the vide-based structural dynamics evaluation. For specific algorithms, the results indicate that both dimensionality reduction techniques and the blind source separation methods play a major role in the mode estimation performance. In the experiment utilizing the cantilever beam structure, all expected modals were successfully identified using the algorithms based on PCA-CP, PCA-ICA, PCA-SOBIRO, PCA-ERICA, NNMF-CP, NNMF-SOBI, NNMF-SOBIRO and NNMF-ERICA. For the second scenario, using the model of a three-story building structure, the methods that correctly perfomed modal analysis are based on PCA-CP, PCA-SOBI, PCA-SOBIRO, PCA-ERICA, NNMF-CP and NNMF-SOBIRO. It is suggested that The effectiveness of combining NNMF and blind source separation methods for modal analysis may be contingent upon the complexity of the system under investigation.

**Keywords**: Video-based Structural Dynamics, Blind Source Separation, Dimensionality Reduction, Modal Analysis.

# Resumo

Compreender as propriedades dinâmicas de um sistema estrutural é indispensável para um estudo confiável do comportamento da estrutura. A identificação da dinâmica estrutural baseada em vídeo tem sido efetivamente usada como um método chave para a análise modal nos últimos anos. Com várias abordagens diferentes, aquelas baseadas na estratégia de separação cega de fontes têm recebido maior atenção para a identificação de características estruturais. A separação cega de fontes aborda o problema de separar ou extrair as formas de onda da fonte original de uma matriz de sensores. Embora a literatura aborde diversas técnicas para realizar a separação de fontes, apenas uma delas (denominada *complexit pursuit*) é frequentemente empregada para soluções baseadas em vídeo. Este trabalho visa explorar outros algoritmos de separação cega de fontes para realizar análise modal baseada em vídeo. Para realizar a decomposição modal, um conjunto de métodos de separação cega de fontes é combinado com diferentes técnicas de redução de dimensionalidade para dinâmica estrutural de alta resolução de campo completo a partir de vídeo. Especificamente, a Análise de Componentes Principais (PCA) e a Fatoração de Matriz Não Negativa (NNMF), técnicas de redução de dimensionalidades, são usadas para compressão de vídeo junto com seis algoritmos de separação de fontes, resultando em doze estruturas diferentes testadas em uma estrutura de viga *cantilever* e um modelo em escala de uma estrutura de edifício de três andares. As técnicas de separação cega de fontes utilizadas são: Complexity Pursuit (CP), Idependent Component Analysis (ICA), Second Order Blind Identification (SOBI), Second Order Blind Identification with Robust Orthogonalization (SOBIRO), Equivariant Robust Idependent Component Analysis (ERICA) e Algoritmo para Extração de Múltiplos Sinais Desconhecidos (AMUSE). As doze técnicas baseadas em algoritmos de redução de dimensionalidade e separação cega de fontes são aqui avaliadas usando como critério de comparação sua forma de modo, coordenadas modais e valores de MAC. O objetivo principal é fornecer uma gama de alternativas para a avaliação da dinâmica estrutural baseada em vídeo. Para algoritmos específicos, os resultados indicam que tanto as técnicas de redução de dimensionalidade quanto os métodos de separação cega de fontes desempenham um papel importante no desempenho da estimativa de modo. No experimento utilizando a estrutura de viga em balanço, todos os modos de vibração esperados foram identificados com sucesso utilizando algoritmos baseados em PCA-CP, PCA-ICA, PCA-SOBIRO, PCA-ERICA, NNMF-CP, NNMF-SOBI, NNMF-SOBIRO e NNMF-ERICA. No segundo cenário, utilizando o modelo de uma estrutura de prédio de três andares, os métodos que realizaram corretamente a análise modal são baseados em PCA-CP, PCA-SOBI, PCA-SOBIRO, PCA-ERICA, NNMF-CP e NNMF-SOBIRO. Sugere-se que a eficácia da combinação de NNMF e métodos de separação cegas de fontes para análise modal pode depender da complexidade do sistema em investigação.

**Palavras-chave**: Análise Dinâmica Baseada em Vídeo, Separação Cega de Fontes, Redução de Dimensionalidade, Análise Modal.

# List of Figures

# List of Tables

# List of abbreviations and acronym

ALS         Alternating Least Squares

AMUSE       Algorithm for Multiple Unknown Signals Extraction

BSS         Blind Source Separation

CP          Complexity Pursuit

DR          Dimensionality Reduction

EMA         Experimental modal Analysis

ERICA       Equivariant Robust Independent Component Analysis

HT          Hilbert Transform

ICA         Independent Component Analysis

NNMF        Non-negative Matrix Factorization

OMA         Operational Modal Analysis

PCA         Principal Component Analysis

PC          Principal Component

SHM         Structural Health Monitoring

SOBI        Second Order Blind Identification

SOBIRO      Second Order Blind Identification Robust Ortogonalization

# Summary

## Bibliography                                                                 43

# 1 Introduction

Civil, mechanical or electrical infrastructures, such as buildings, bridges, dams, wind turbines and piping systems are exposed to various external stresses throughout their life cycle. Vibrations caused by earthquakes, wind, temperature, or human excitation can cause structural damage and subsequent catastrophic failure. Structural Health Monitoring (SHM) usually refers to the process of implementing a damage detection and disaster mitigation strategy for physical structures [1]

The SHM comprises four key elements: data acquisition, system identification, condition assessment and decision making/maintenance [2]. This process involves the observation of a structure or a system over time using periodically spaced dynamic response measurements, the extraction of damage-sensitive features from these measurements and the statistical analysis of these features to determine the current state of system health. Therefore, dynamic characteristics of a structure must be extracted to better understand structural vibrational problems.

Modal Analysis is the process whereby it is possible to describe a system in terms of its dynamic characteristics, such as natural frequencies, damping ratios and mode shapes, which later can be used to formulate a mathematical model of the dynamic behavior. Over the past two decades, it has become an essential tool in the quest to resolve vibration-related problems in machines and structures [3].

The dynamic characteristics of a structure can be comprehensively defined by its the natural frequencies and mode shapes. The mode dynamics are inherent properties of structures and are related to structural resonances (they vary with changes in geometry, material properties, and boundary conditions, for example). Natural frequencies depend on the material, its density, and the damping of the system. Every system has a set of natural frequencies and resonance occurs when the frequency of an external load equals one of them. It may cause vibration at dangerously high amplitudes.

These modal parameters must be identified to fully determine the dynamic behavior of the structure. Consequently, it is imperative that the technique and device used for performing modal analysis are practical, not labor intensive, cost-effective and can be easily used for real applications.

Currently, there are two main modal analysis techniques: experimental modal analysis (EMA) and operational modal analysis (OMA) [4]. EMA is the oldest modal analysis technique and it is performed in controlled laboratory environment for an artificially excited structure. OMA, on the other hand, is performed while the structure is in operation [5, 6] . The paradigm of EMA and OMA techniques will be briefly discussed in the next section and then vision-based approches for modal analysis will be presented.

## 1.1    Context

A tradidional issue about EMA and OMA is the requirement for physically-attached wired or wireless sensors for vibration measurement of structures [7]. This instrumentation can result in mass-loading on lightweight structures, and is costly and time-consuming to install and maintain on large civil structures, especially for long-term applications (e.g., structural health monitoring) that require significant maintenance for cabling (wired sensors) or periodic replacement of the energy supply (wireless sensors). For these reasons, non-contact measurements, mainly the ones based on video recordings, have received intensive research efforts in the last few years due to their extremely high spatial sensing resolution (i.e., each pixel is treated as a single motion detector, and a potential diminute sensor), relatively low-cost and agile, simultaneous, measurements. Combined with vision-based algorithms (e.g., image correlation, optical flow), video-based measurements have been successfully used for vibration measurements and subsequent modal analysis[8, 9, 10, 11, 12].

Modal analysis frameworks based on dimensionality reduction and decomposition algorithms have been applied to perform vide-based modal identification sucessfully. They focus on acomplishing the structural system identification [11, 13, 14] . In general, decomposition algorithms refer as a solution to a problem where both the sources and the mixing mechanism are unknown, only mixture signals are available for further separation process. Thus, they are a powerful tool for signal analysis, because they can decompose signals into several narrow-band components, which is advantageous to quantitatively evaluate signal characteristics. Blind source separation is a class of unsupervisioned methods that has been developed and applied as decomposition algorithms [15, 16].

In the field of structural dynamics, in particular, blind source separation (BSS) techniques are proeminent, allowing to blindly perform output-only modal identification [17]. However, the application of dimensionality reduction algorithms over the number of measurements is commonly required when applying BSS algorithms. Amid these compression techniques, principal component analysis (PCA) and nonnegative matrix factorization (NNMF) stand out [18, 19].

As PCA is often applied to reduce the dimensionality of the data, its principal components are closely related to the modal components of the structure, with the advantage of preserving the full-field resolution vibration information [12]. NNMF also achieve dimensionality reduction and motion decomposition by blindly identifying independent components. For this, the sources must be statistically dependent under conditions that impose additional constrains as non-negativity and sparsity [20]. Later, after chosing one particular technique for dimensionality reduction, BSS is carried out for modal analysis.

Due to its popularity, several works have explored BSS methods for structural dynamics. Musafere (2016) explores damage detection using BBS integrated with time varying auto-regressive modeling [21]. The second-order blind identification algorithm (SOBI) solves the blind source separation problem. The technique is employed first to obtain the mono-harmonic responses from the vibration data, and then the discrete changes in the natural frequencies identify the instant and severity of damage.

Cheng (2016) analyses two different BSS algorithms, independent component analysis (ICA) and SOBI, for the condition monitoring of dams. The SOBI-based modal identification is suited to determine the system orders, while ICA calculates modal features to detect structural damage and determine the location of it [22]. Output-only modal analysis using ICA and SOBI is also studied by Poncelet (2007). Here, the concept of virtual source is exploited and renders the application of these BSS techniques possible [23].

Li (2020) approaches a case of operational mode analysis under a limited number of sensors. The work compares the results using only SOBI to the results using a proposed frequency domain blind identification method called FSOBI. The proposed method is a combination of the joint diagonalization of a set of weighted covariance matrix and the second-order BSS technique.[24]

Zhou and Chelidze (2007) proposed a novel method for linear normal mode identification based on BSS. The modal idetification were performed by two well-known BSS algorithms. First, the algorithm for multiple unknown signals extraction (AMUSE) is examined in detail and compared to a well-known time domain modal analysis method. Second, SOBI is used to demonstrate noise robustness of BSS-based mode shape extraction [25].

Wang (2016) aimed at the problem of lack of comparison and evaluation of different ICA algorithms for output-only modal analysis [26]. Different objective functions and optimization methods of ICA are explored. Simulation results on simply supported beam verify the effectiveness, robustness, and convergence rate of five different ICA algorithms for output-only modal parameters identification. it is shown that the one based on the quasi-newton iterative method [27, 28] is more suitable for modal parameter identification among the ICA algorithms considered.

A study about the second-order blind source separation (SOBSS) algorithms for OMA is introduced by Antoni (2013). It is conducted a theoretical analysis of SOBSS methods applied within the OMA framework. It is also proposed a new separation method to fix the limitations AMUSE and SOBI have shown, such as the inability to deal efficiently with additive noise at zero time-lag and to estimate complex mode shapes [29].

Antoni (2017) approaches an interpretation and generalization of complexity pursuit (CP) for the blind separation of modal contributions. It states that CP is another BSS problem and it is found to separate components which are the least dispersive (i.e. invariant under linear filtering), a property that well characterizes the modal responses of lightly damped systems. CP is presented as a strong analogy with AMUSE, the two time-lag version of SOBI [30].

Thereby, several decomposition algorithms are proposed on the literature for modal analysis: ICA, SOBI, SOBIRO, AMUSE, ERICA, CP. Thus, dimensionality reduction and decomposition algorithms have been successfully applied in video-based modal identification for structural system identification. Blind source separation techniques, including principal component analysis and non-negative matrix factorization, have been used for output-only modal identification in the field of structural dynamics. Several studies have explored BSS methods for structural dynamics, including damage

detection, condition monitoring, and mode shape extraction. Novel methods for linear normal mode identification have also been proposed based on BSS algorithms. These studies demonstrate the potential of BSS techniques for modal analysis in structural dynamics, and suggest that they can be powerful tools for signal analysis and separation.

## 1.1.1 Non-contact Vision-based Approaches for Modal Analysis

State-of-the-art video-based structural dynamics identification methods are able to blindly perform modal analysis from video measurements of vibrating structures, without any additional surface preparation. Structural vibration can be measured into video recording containing frames with temporally displaced image intensities. In the recently proposed analysis solutions, a digital video camera provides very high spatial resolution measurements and every pixel effectively becomes a measurement point on the structure. These techniques attain full-field high-resolution mode shapes and modal coordinates, which in turn, are required to estimate resonant frequencies and damping ratios.

Non-contact vision-based techniques for identification of structural dynamics have the advantage that they are less expensive to deploy compared to tradional techniques, such as the use of accelerometer or strain gauge. In order to these techniques get acknowledgment, it is expected to develop modal analysis methods based on video camera measurements only without additional strucutral surface. Full-field, high-resolution, unsupervised learning-based strucutral dynamics identification frameworks based on decomposition algorithms (PCA and BSS, for example) can make use of digital video cameras that are relatively low-cost and agile and provides very high spacial resolution measurements [8, 10].

For scenarios using vision-based approaches, in particular those whose techniques require no surface preparation, BSS also plays an important role. Yang (2017) proposed an efficient novel operational modal analysis method combining multi-scale pyramid decomposition and the complexity pursuit (CP) algorithm as a BSS technique [8]. The method manipulates the spatio-temporal pixels phases that encode the local structural vibration in the video measurement, being capable to blindly identifying the modal frequencies, damping ratios and high-resolution mode shapes. Martinez (2020) proposed a full-field, high-resolution, structural dynamics identification bsss-based framework coupled with compressive sampling [10]. In both works, phase-based optical flow converts each pixel intensity to displacement and results in a time series for every pixel. The PCA is applied across all of the displacement time series to reduce the dimensionality of data, while the system identification is accomplished by solving the BSS problem.

Silva (2020) approaches the problem of video-based modal identification associating NNMF and BSS solved by CP. The method also explores the timing information present in the pixel time-series to infer spatial relationships and, thus, blindly estimate modal parameters. The main difference between the aforementioned approach and the ones using phase-based optical-flow is that the later one is directly applied over the raw pixel time-series without any pre-processing step, such as the phase-based optical flow estimation. By using nonnegative matrix factorization, a spatio-temporal decom-

position is achieved over the pixel time-series directly [12].

Later, Silva (2022) proposed adapted its technique for applications involving the estimation of travelling waves and complex mode shapes from video measurements. That generalized technique improves the decomposition results of the previous techniques by using the Hilbert Transform for augmenting the video data to obtain phase information. From the augmented dataset, PCA and BSS are applied to estimate real and imaginary modes, being capable of suitably decompose individual travelling wave sources into their fundamental components [31].

## 1.2   Problems and Motivations

The level of complexity of structures has increased along with the demand for better and on-going assessment of structures over the past years. New monitoring capabilities that enable quick and responsive assessment are needed, such as online data collecting, high-resolution measurements, and time-efficient data processing. As an efficient solution, the modal analysis performed using only videos can apply blind source separation and dimensionality reduction as their principal steps.

Although the literature addresses several BSS techniques, only CP algorithm has been often employed for non-contact video-based modal analysis. The structural dynamics community, however, applies a variety of other BSS solutions that may be useful in this scope. This issue is tested here to provide a range of alternatives for the video-based structural dynamics evaluation.

Thus, the theoretical relevance of this work is to fulfill the lack of studies using other BSS techniques to perform video-based EMA. In practice, the purpose of this study is to contribute to the video-based structural dynamic field assisting the choice of the dimensionality reduction algorithms and providing options to the blind source separation-based approaches for video.

In addition, the motivation and interpretation of the dimensionality reduction step are relevant. PCA and NNMF have been successfully used in this step. It is interesting to study how they perform combined with different BSS techniques.

Comparing BSS and also dimensionality reduction methods is experimentally feasible in the context. To demonstrate the proposed approach, EMA is conducted on a bench-scale building structure and a cantilever beam, for which accelerometers are used to validate the extracted modal parameters.

## 1.3   Objectives

This work aims to provide a general understandment about the BSS algorithms applying to the non-contact vision-based approaches for experimental modal analysis. The goal is to explore and compare a set of BSS algorithms combined with dimensionality reduction methods for full-field high-resolution structural dynamics from video. The algorithms used for modal identification from video

of vibrating structures (without surface preparation) are based on the combination of decomposition algorithms (PCA and NNMF) with six different BSS techniques. Thereafter, the results are shown based on the extracted mode shapes and modal coordinates.

EMA is perfomed by an algorithm wih three main steps: Pre-processing, dimensionality reduction and blind source separation. The association of thechniques proposed to achieve the second and third steps provides twelve different methods for video-based structural dynamic analysis. This work specifically aims to apply each of them in two different structures. So, based on the dynamic characteristics of the systems (modal coordinates and shape of the modes) and on the Modal Assurance Criterion (MAC), it is possible to establish a comparative scenario between the twelve proposed techniques.

### 1.3.1   Specific Objectives

- Implement six algorithms based on PCA and BSS techniques to perform full-field high-resolution structural dynamics analysis from video;

- Implement six algorithms based on NNMF and BSS techniques to perform full-field high-resolution structural dynamics analys from video;

- Determine de mode shapes and modal coordinates from a video of a cantilever beam subjected to excitations;

- Determine de mode shapes and modal coordinates from a video of a bench-scale model of a three-story building structure subjected to excitations;

- Compare and analyse the modal identification to each structure based on the mode shapes, modal coordinates and the modal assurance criterion.

## 1.4   Organization of this work

This work is organized in five chapters to present the theoretical framework of the problem, the methodology and the results.

**Chapter 2** defines dimensionality reduction and explain two famous techniques used to perform that. It also presented the blind source separation problem along with six different algorithms that are used in the SHM field as a solution.

**Chapter 3** presents the methodology applied to perform modal analysis for full-field high-resolution structural dynamics from video. An outline of the method conducted for modal identification from video of vibrating structures is presented. It includes the pre-processing steps, the dimensionality resduction and the blind source separation process applied to find the dynamic properties of structures.

**Chapter 4** shows the results of full-field vision-based techniques for output-only modal analysis with application on laboratory structures to decomposing vibration modes in lab-scale physical structures.

**Chapter 5** draws the conclusions and points out some future work.

# 2 Dimensionality Reduction and Blind Source Separation

Chapter 1 introduced previous works on the structural dynamics field, specially the video-based frameworks that utilize the video measurments only, without additional structural surface preparation. They have shown proeminet techniques to visualize and process high-dimensional data and to indentify the mode shapes, modal coordinates and damping ratios. As mentioned in the last chapter, dimensionality reduction and blind source separation are compelling tools to perform full-field high-resolution structural dynamics analysis from videos.

With the proper context of the structural dynamics analysis presented in the previous chapter, it is imperative to proceed to the dimensionality reduction (DR) problem. This chapter is intended to intoduce key concepts and an overview of two distinct approaches to DR of the data. It is often useful to reduce the dimensionality by identifying sets of uncorrelated variables that explain most of the variability of the data.

This chapter also discusses about another major step to perform vide-base modal analysis: blind source separation. This work summarizes six different techniques used in the structural dynamic field, although there are many other methods to resolve the BSS problem.

## 2.1  Dimensionality Reduction

Real-world data for engineering applications usually have high dimensionality and variables that depend on the value assigned to each other. Observations are described by several dependent variables which are, in general, intercorrelated and include noise. To adequately process such data, its dimensionality must be reduced. Dimensionality reduction is the transformation of high-dimensional data into a small subset of independent variables. Ideally, the dimensionality of the reduced representation should match the inherent dimensionality of the data. The intrinsic dimensionality of the data is the minimum number of parameters required to account for the observed properties of the data. Dimensionality reduction is important, not only for SHM, but also in many fields because it alleviates the curse of dimensionality and other undesirable properties of high-dimensional spaces as well as reduces the computational load in processing. Therefore, dimensionality reduction facilitates the classification, visualization, and compression of high-dimensional data [32, 33].

In general, the goal of DR is to find lower dimensional representations of data that preserve their key properties for a given problem. Mostly, the classical technique to DR was principal component analysis, referred to as PCA. In general, choosing the DR technique depends mostly on the

problem being solved [33].

## 2.1.1 Principal Component Analysis (PCA)

PCA was originally introduced by Pearson [34] and developed independently by Hotelling [35] who also introduced the term *principal component*. Principal component analysis is a linear dimension reduction technique, which is effective for visualizing high dimensional data and for data pre-processing. PCA is an unsupervised linear mapping based on an eigenvector search and suitable for Gaussian data. It provides different strategies for reducing the dimensionality of feature space and preserves the maximum amount of variance of the original data [36]. That is to say the central idea of the PCA is to reduce the redundancy of data under the assumption that, in terms of information, some dimensions are more important than others.

Fundamentally, PCA reduces the dimensionality (i.e., the number of variables) of a data set by maintaining as much variance as possible. The technique reduces the number of input variables in a dataset into a small number of meaningful variables. It is an amenable dimensionality reduction technique for orthogonal sources, especially when the most interesting sources have the largest variances.

PCA computes a set of new orthogonal variables, so called principal components (PCs). Data are reduced by geometrically projecting them onto lower dimension PCs. The goal is to find the best summary of the data using a limited number of them. They are obtained as linear combinations of the original variables. The first one is chosen to minimize the total distance between the data and their projection onto the PC. By minimizing this distance, the variance of the projected points is maximized, $\sigma^2$. The subsequent PCs are selected similarly, with the additional requirement that they have to be uncorrelated with all previous PCs. That requirement of no correlation means that the maximum number of PCs possible is either the number of samples or the number of features, whichever is smaller[37, 38].

Follow the steps of the PCA to reduce the dimension of a $m$-dimensional dataset given by $\boldsymbol{x(t)} = [x_1(t), ..., x_m(t)]$ [39] [40].

- *Step 1*: Calculate the mean ($\alpha$) of the data. For PCA to work properly, it is necessary to subtract the mean from each of the data dimensions. The mean subtracted is the average across each dimension.

$$\alpha = \frac{1}{m} \sum_{i=1}^{m} x_i. \tag{2.1}$$

- *Step 2*: Use the generated mean to calculate the covariance matrix $\sum$ of the sample set, such as:

$$\sum = \frac{1}{n} \sum_{i=1}^{m} (x_i - \alpha)(x_i - \alpha)^T. \tag{2.2}$$

The diagonal values of the covariance matrix represent the variance of the variable $x_i$, $i = 1, ..., m$, while the off-diagonal entries represent the covariance between two different variables.

$$\sum = \begin{bmatrix} Var(x_1, x_1) & Cov(x_1, x_2) & \cdots & Cov(x_1, x_m) \\ Cov(x_2, x_1) & Var(x_2, x_2) & \cdots & Cov(x_2, x_m) \\ \vdots & \vdots & \ddots & \vdots \\ Cov(x_m, x_1) & Cov(x_m, x_2) & \cdots & Var(x_m, x_m) \end{bmatrix}. \tag{2.3}$$

A positive value in covariance matrix means a positive correlation between the two variables, while the negative value indicates a negative correlation and zero value indicate that the two variables are uncorrelated or statistically independent.

- *Step 3*: Calculate the eigenvectors $V$ and eigenvalues $\lambda$ of the covariance matrix.

$$V \sum = \lambda V. \tag{2.4}$$

Eigenvectors are non-zero vectors and eigenvalues are scalar. Each eigenvector represents one principal component and each corresponding eigenvalue represents the scaling factor, length, magnitude, or the robustness of the eigenvectors. Therefore, the eigenvector with the highest eigenvalue represents the first principal component and it has the maximum variance.

- *Step 5*: Select the eigenvectors that have the largest eigenvalues $W = (v_1, ..., v_k)$. The selected eigenvectors (W) represent the projection space of PCA. To construct the PCA space, a linear combination of $k$ selected PCs that have the most significant $k$ eigenvalues are used to preserve the maximum amount of variance, i.e. preserve the original data, while the other eigenvectors can be neglected. The positions of each observation in this new coordinate system of principal components are called scores, the data projected onto the PCA space. See Figure 1.
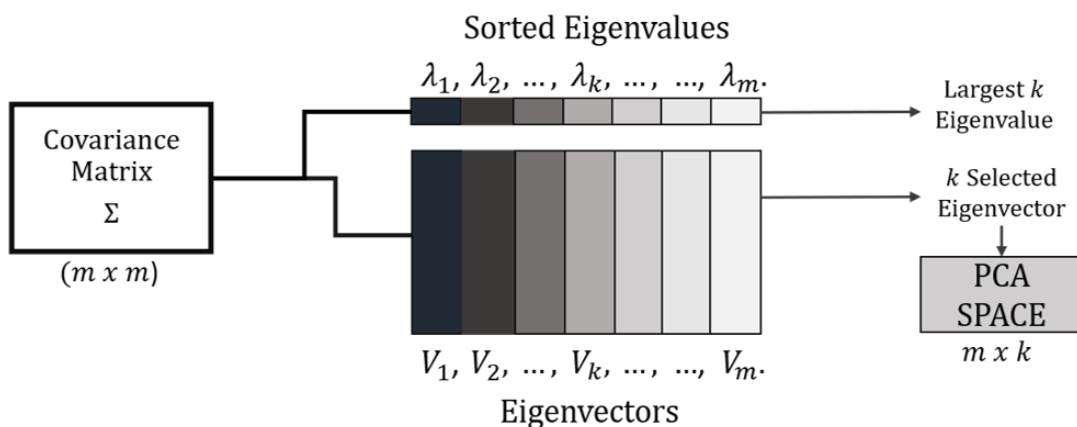


Figure 1 – Construction of the PCA space. The eigenvectors and eigenvalues are found from the covariance matrix. The eigenvectors are sorted by the largest $k$ eigenvalue to map each row of the dataset to a new vector of principal component scores. Source: own elaboration.

In general, once eigenvectors are found from the covariance matrix, the next step is to order them by them eigenvalues, from highest to lowest. This provides the components in order of significance. Now, it is possible to decide to ignore the components with lower importance. Of course the system loses some information, but as the eigenvalues are small, in most cases, that is negligible. If some components are omitted, the dimensionality of the final dataset will be smaller than the original dataset.

- *Step 6*: Deriving the new dataset $y$. The dimension of the original data is reduced by projecting it after subtracting the mean onto the PCA space as follows:

$$y(t) = \sum_{i=1}^{m} W^T (x_i - \alpha). \tag{2.5}$$

The original data are projected on the PCA space, and then the PCA reduces the dimension from $m$ to $k$.

## 2.1.2   Nonnegative Matrix Factorization (NNMF)

As an alternative for DR, the nonnegative matrix factorization can be employed in the context of video applications. It is a spatio-temporal method to reduce data dimension. This method has become a widely used tool for the analysis of high-dimensional data as it automatically extracts sparse and meaningful features from a set of nonnegative data vectors [41]. Due to its nonnegative constraint NNMF is extremely suitable for video processing (i.e., the pixel values are RGB intensities), among other applicaitons. The reason why NNMF has become so popular is because of its ability to automatically extract sparse and easily interpretable factors [42, 43, 44, 45, 46].

NNMF decomposes $\mathbf{V} \in \mathbb{R}^{m \times n}$, a matrix contained the high-dimensional data wich all entries are nonnegative values only, into two nonnegative matrices $\mathbf{W} \in \mathbb{R}^{m \times k}$ and $\mathbf{H} \in \mathbb{R}^{k \times n}$ whose product provides a good approximation to the original matrix. $\mathbf{W}$ acts as a dictionary of recurring patterns, regarded as the basis vectors. The dimensionality reduction is performed by projecting $\mathbf{H}$ onto the lower dimensional space that is formed by basis vectors.

NNMF is, in fact, a multivariate data analysis. Let matrix $\mathbf{V}_{m \times n}$ be the data matrix with $n$ samples in $m$-dimensional space and all elements of the matrix be nonnegative ($\mathbf{V} \geq 0$). The matrix can be linearly decomposed into

$$\mathbf{V}_{n \times m} \approx \hat{\mathbf{V}} = \mathbf{H}_{n \times k} \mathbf{W}_{k \times m}. \tag{2.6}$$

$\mathbf{H}_{m \times k}$ is called basis matrix and $\mathbf{W}_{k \times n}$ is called coefficient matrix. . It leads to dimensionality reduction when using $k$ smaller than $m$ and considering the coefficients as new features, and to lower storage and computational resources [12].

Figure 2 exemplify the result of NNMF applied to a video of a bench-scale building. Note that in the case of the videos of vibrating strucutres, the NNMF is applied over the pixel time-series contained in $\mathbf{V}$. Therefore, the extracted components in $\mathbf{W}$ accounts for a temporal decomposition with each column $\mathbf{W_i}$, indicating the time pattern of a specific vibration mode. On the other hand, $\mathbf{H}$ incorporates a spatial decomposition with each row $\mathbf{h_i}$, when properly reshaped, resembling the corresponding vibration mode shape. Thus, considering both $\mathbf{W}$ and $\mathbf{H}$ there is a spatio-temporal decomposition.

Some algorithms have been proposed for the NNMF problem. The first algorithm proposed for solving the nonnegative matrix factorization was the alternating least squares method [47]. Later, Lee and Seung suggested the multiplicative rules, one of the most popular algorithm for NNMF [42]. Also, considering the non-negative matrix factorization as a nonlinear optimization problem on a convex set, Lin (2007) proposed an class of algorithms based on gradient descendent [48].

For the purpose of the structural dynamic analysis in this work, the basic alternating least squares (ALS) method are explored. The ALS combines a least squares step followed by another least squares step in an alternating fashion. The algorithm exploits the fact that the optimization of both $\mathbf{W}$ and $\mathbf{H}$ is not convex, and thus ill-posed, i.e. problems whose solutions are not unique and depends on the initial values. However, solving for either $\mathbf{W}$ or $\mathbf{H}$, separately, leads to a convex optimization. Thus, given one matrix at a time, the other matrix can be estimated with trivial least squares computations [12, 42, 49].
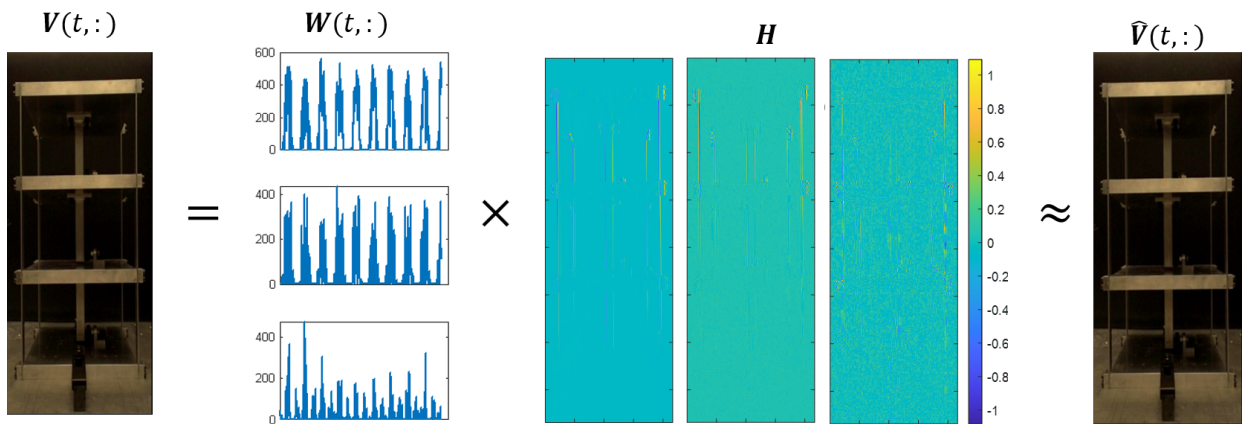


Figure 2 – Example of a NNMF algorithm applied to a pixel time-series matrix for DR using a video of a bench-scale building structure. NNMF decomposes $\mathbf{V}$ into two nonnegative matrices $\mathbf{W}$ and $\mathbf{H}$ and the product provides a good approximation of the original matrix. Source: own elaboration.

## 2.2   Blind Source Separation

The earliest substantive study about blind source separation dates back 1986 by Herault and Jutten at a Neural Network Conference. The authors presented the H-J algorithm, a feedback neural network model with a hebb-based learning algorithm, to separate two mixed statistically independent source signals [50]. This work opened a new chapter in the field of signal processing, and, since then,

the BSS problem has attracted extensive attention from scholar [51]. Over the last decade, the BSS problem still a hotspot in signal processing with a applicaton in many fields, such as neuroscience [52, 53], audio processing [54, 55], data analysis in geophysical exploration [56, 57] and speacially in the structural dynamics field [12, 22, 24, 58].

The BSS problem consists in separating a set of original signals $s(t)$ , called sources, from a multivariate set of $x(t)$ mixed signals, called mixtures, without the aid of information about the sources or the mixing process. To accomplish such a separation, one can use several implicit features on the sources. The term "blind" is intended to imply that such methods can separate data into source signals only from the mixed signals, knowing nothing about the nature of the source signals [18, 59].

A general BSS problem can be formulated as follows [60]:

$$x(t) = As(t) = \sum_{i=1}^{j} a_i s_i(t).$$ 
(2.7)

The function $x(t)($ is the records of sensor signals, $x(t) = [x_1(t), ..., x_m(t)]^T$, from a multiple-input/multiple-output system. The objective is to find an a unmixing system, if it exists and is stable, in order to estimate the $j$ source signals $s(t) = [s_1(t), ..., s_j(t)]^T$ or only some of them with specific properties. This estimation is performed on the basis of only the output signals $y(t) = [y_1(t), ..., y_j(t)]^T$ and the sensor signals; $A \in \mathbb{R}^{m \times j}$ is an unknown matrix consisting of $j$ columns with its $i^{th}$ column $a_i \in \mathbb{R}^m$ associated with $s_i(t)$. Figure 3 shows the general signal processing model for the BSS problem where multiple unknown sources are combined together by some unknown mixing system to produce a set of observations, where each observation is a mixture of the sources [61].
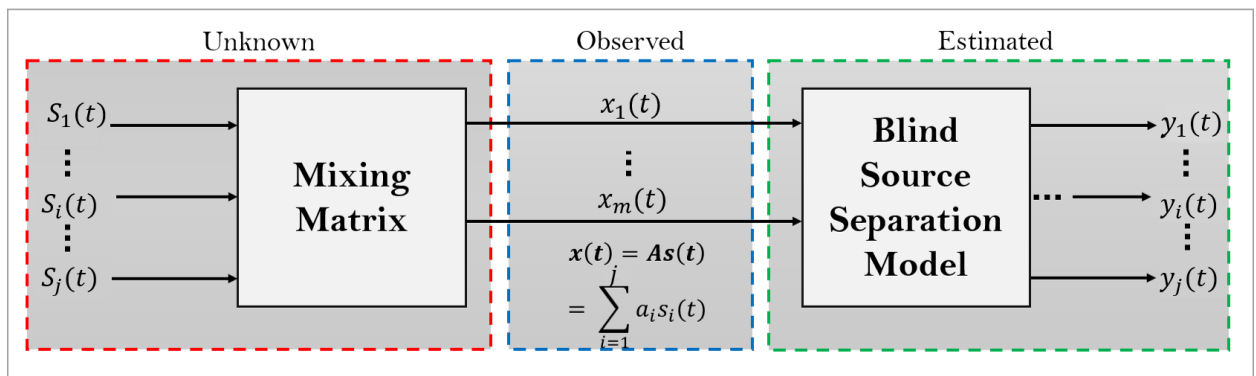


Figure 3 – Blind source separation problem. A group of unknown sources are mixed together to produce a set of observed mixture signals. A source separation algorithm (and its associated demixing operation) estimates the sources.Source: own elaboration.

The problems of separating or extracting the original source waveforms from the sensor array, without knowing the transmission channel characteristics and the sources can be expressed briefly as a number of related BSS problems such:

1. Complexity Pursuit (CP)

2. Independent Component Analysis (ICA)

3. Second Order Blind Identification (SOBI)

4. SOBI Robust Ortogonalization (SOBIRO)

5. Equivariant Robust ICA (ERICA)

6. Algorithm for Multiple Unknown Signals Extraction (AMUSE)

## 2.2.1 Complexity Pursuit

The complexity pursuit idea is based on finding the projections $\boldsymbol{w}^T\boldsymbol{x}(t)$, assuming the observed data as multivariate time series $\boldsymbol{x}(t)$, such that the Kolmogoroff complexity [62]of the projection is minimized.This is a general-purpose measure and is probably connected information-processing principles used in the brain [11, 63, 64, 65].

It is an approximation of the Kolmogoroff complexity of a zero mean scalar signal $(t)$ along similar lines as Tang (2005) and Hyvarinen (2001). The value $\boldsymbol{y(t)}$ is predicted from the preceding values by some function $f$ given by:

$$f(\boldsymbol{y(t)}) = \sum_{\tau=1}^{L} \alpha_\tau f(y(t-\tau)) + \delta y(t), \qquad (2.8)$$

where $\tau$ is a specific time delay, $L$ is the degree of the predicting model, $\alpha_\tau$ is a predicting parameter and f is a differentiable function which defines the linear or nonlinear predictor structure of the signal. Generally, the choice of the function $f$ is based on statistical properties of primary sources.

## 2.2.2 Independent Component Analysis

Independent component analysis is a statistical technique for signal separation. ICA is used to decompose a multivariate signal into decomposing a multivariate signal into additive subcomponents. Each component is a representation of one of the underlying sources of information in the signal. ICA is based on the simple, generic and physically realistic assumption that if different signals are from different physical processes (e.g., different people speaking) then those signals are statistically independent [66, 67].

There are two key assumptions made in ICA. The hidden independent components must be one, statistically independent, and two, non-Gaussian. Semantically, by independent, it means information about $x_1$ does not give any information about $x_2$ and vice versa.

ICA is particularly useful for separating mixed signals that have been contaminated by other signals. For example, ICA can be used to remove background noise from an audio signal [68] or to isolate the different types of activity in an magnetic ressonance imaging data set [69].

The goal of ICA is to find a linear transformation of the data that maximizes the independence of the resulting components. This is done by finding a matrix $\boldsymbol{W}$ that minimizes the overall correlation between the columns of $\boldsymbol{W} \cdot \boldsymbol{x}$, given $\boldsymbol{x(t)}$ as the data matrix.

The result of ICA is a set of independent components, which can be thought of as the underlying sources of variability in the data. These components can be further analyzed to identify their structure and function.

ICA is a powerful tool for separating signals, but it does have some limitations. One limitation is that ICA cannot handle non-linear relationships between sources. Another limitation is that ICA assumes that the number of sources is known ahead of time.

## 2.2.3   Second Order Blind Identification

The SOBI algorithm is based on the approximated joint diagonalization of two correlation matrices with different delays. Given a whitened vector $\boldsymbol{z[n]}$ a set of $r$ delayed correlation matrices of $\boldsymbol{z[n]}$, $\boldsymbol{R_z}\left(\tau_i\right)$, $i = 1, ..., r$ is considered. The SOBI aims at finding a unitary transformation $\mathbf{V}$ such that:

$$\boldsymbol{V}^T \boldsymbol{R_z}(\tau_i)\boldsymbol{V} = \boldsymbol{D}_i, \tag{2.9}$$

here, $\boldsymbol{D}_i$ is a set of covariance matrices of the estimated signal $\boldsymbol{y(t)}$.

Since the SOBI works with several correlation matrices, it reduces the probability that an incorrect choice of the delay will prevent the implementation of blind separation. Experiments have shown that the use of several correlation matrices in environments where there is a low SNR and/or sources with a small spectral difference is more efficient and robust [70, 71, 72, 25].

## 2.2.4   SOBI Robust Orthogonalization

SOBIRO is a variant of SOBI using a robust orthogonalization method. . Belorachrin and Cichocki (2000) [73] presented a robust technique applied in the pre-step *whitening* called Robust Orthogonalization that can give us a better estimation of the coefficients of the whitening matrix $\boldsymbol{W}$ [70, 74].

Given the a dataset $\boldsymbol{x(t)}$ from unkown sourcers and $\boldsymbol{A}$ the unknowing mixing matrix that make the data $\boldsymbol{x(t)}$ a linear combination of the unknown sources $\boldsymbol{s(t)}$, then pre-step of robust orthogonalization ensures that the resulting estimate is not sensitive to small perturbations in the data. In the Robust Whitening, a set of covariance matrices of $\boldsymbol{x(t)}$ at different lags is used to estimate the whitening matrix:

$$\boldsymbol{R_x}(\boldsymbol{\tau}) = E[\boldsymbol{x(t)} \cdot \boldsymbol{x^*(t - \tau)}] = \boldsymbol{A}\boldsymbol{R_S}(\tau)\boldsymbol{A}^H, \tag{2.10}$$

where $\tau = 1, ., k$

The method uses an optimization algorithm that estimate a linear combination of evaluated covariance's matrices $\boldsymbol{R}_x$:

$$\boldsymbol{C} = \sum_{\tau=1}^{k} \alpha_\tau \hat{\boldsymbol{R}}_x(\tau). \tag{2.11}$$

The eigenvalue decomposition of $\mathbf{C}$ is performed:

$$\boldsymbol{C} = \boldsymbol{U_C} diag[{\lambda_1}^2, ..., {\lambda_n}^2]U^T{}_C. \tag{2.12}$$

And, finally, the whitening matrix is:

$$\boldsymbol{Z} = diag[{\lambda_1}^2, ..., {\lambda_n}^2]^{-1}U^T{}_C. \tag{2.13}$$

Then, the whitened data $\mathbf{z}$ is espressed as:

$$\boldsymbol{Z} = \boldsymbol{W}.\boldsymbol{A}.\boldsymbol{x} \tag{2.14}$$

## 2.2.5   Equivariant Robust ICA

Equivariant Robust Independent Component Analysis is an algorithm based on cumulants. The technique (which is asymptotically equivariant in the presence of Gaussian noise) has been developed by Sergio Cruces, Luis Castedo and Andrzej Cichocki [75]. This algorithm separates the signals from $m$ mixture of $n$ sources (with non-zero kurtosis) in the presence of Gaussian noise. This algorithm is a quasi-Newton [28] iteration that will converge to a saddle point with locally isotropic convergence, regardless of the distributions of the sources. The use of prewhitening is not necessary for this algorithm to converge [76].

ERICA is an extension of the well-knownIndependent Component Analysis (ICA) algorithm, which is a type of blind source separation algorithm. Equivariant ICA can be used in cases where the data is not linearly separable, or when there are non-Gaussian distributions present. In addition, equivariant ICA is robust to outliers and noise, making it a good choice for applications where the data may be corrupted.

## 2.2.6   Algorithm for Multiple Unknown Signals Extraction

AMUSE was introduced by Tong et al. in 1990 [77] and can handle Gaussian sources. AMUSE exploits the second-order statistics of the mixed signals and performs an eigenvalue decomposition to the time-lagged covariance matrix. That is, AMUSE algorithm is a type of second-order decorrelation based BSS algorithm [78]. The main advantage of AMUSE is that it sorts the components automatically due to application of PCA [79].

AMUSE employs PCA two times in cascade way for pre-whitening and separation respectively following two stages:

- First, as soon as the samples of $s(t)$ are obtained, the covariance matrix is computed $R = [s(t)s^T(t)]$.Then, an eigenvalue decomposition is performed on $R$ to a whitening matrix $H$. Then the whitened signal $\overline{s}(t)$ is calculated by:

$$\overline{s}(t) = Hs(t). \tag{2.15}$$

- Second, compute the time lapse covariance matrix of the signal $\overline{s}(t)$. Then, perform the singular value decomposition of the covariance matrix to estimate the source signals.

The table 1 summarizes the main advantages and disadvantages regarding the mentioned BSS methods.

| Algorithm | Advantage | Disadvantage |
| --- | --- | --- |
| CP | Well-known algorithm for non-contact vision-based modal analysis. | Prone to local minima and sensitive to initialization parameters. |
| ICA | Can separate sources with non-Gaussian distributions. | Requires statistical independence between sources, which may not always hold in real-world scenarios. |
| SOBI | Robust to noise and can separate sources with any distribution. | Assumes that the sources are linearly mixed, which may not always hold in real-world scenarios. |
| SOBIRO | Can handle a large number of sources and is robust to noise. | Computationally expensive and requires estimation of high-dimensional covariance matrices. |
| ERICA | Can handle non-linear mixing and is robust to outliers. | Requires a priori knowledge of the group action on the sources, which may not always be available. |
| AMUSE | Can handle non-stationary sources, it is robust to noise and sorts the components automatically | Requires knowledge of the number of sources and is sensitive to the choice of the sparsity-promoting penalty. |

Table 1 – Main advantages and disadvantages of the BSS algorithms

The next chapter presents an output-only modal analysis framework based on the dimensionality reduction and BSS techniques and the use of these techniques specifically for full-field high-resolution modal identification from videos of vibrating structures.

# 3  Modal Identification from videos of Vibrating Structures

This chapter addresses an overview of the methods applied for video-based structural dynamics identification. Figure 4 summarizes the output-only modal analysis framework for extracting full-field high-resolution modes from video of vibrating structures. The major three steps are pre-processing, on the basis of the Hilbert Transform for phase extraction, dimensionality reduction and blind source separation.

The video-reshaping and pre-processing step aims to extract the relevant phase-series from the video of the structure. Later, the dimensionality reduction and blind source separation steps perform the structural system identification.

## 3.1  Video Reshaping and Pre-Processing

The temporal aspect linked to the pixel time-series of video recordings holds crucial data on spatial differences. Yang et al. [8] showed that when each pixel is treated as sensor for the prospective motion detector, the spatial resolution of video-based modal analysis can be significantly enhanced. Then, the first step of the framework is reshape the input video to form pixel-wise time-series for futher process. It is important to emphasize and resume that the video is not processed frame by frame. In fact, each pixel is related to a time-series that maps the temporal displacement across the time-span of the video. In this way, an amount of time series equivalent to the video resolution is the data that contains the structural dynamics information. Thereby, each pixel effectively becomes a measurement point and the number of time series is equals the spatial resolution of the video.

The pre-processing component is the application of the The Hilbert Transform (HT) before the DR perfomed by PCA. HT is a technique that can be used to turn a signal into an analytic signal. The analytic signal contains both the original and the Hilbert Transform of the signal. The HT of a signal is the signal that would result after it is shifted by 90 degrees in the complex plane. This is a very powerful tool as the result contains all the information of the original signal plus the information of the Hilbert Transform phase. The main advantage is to perform many operations that would not be possible with the original signal [80, 81].

The Hilbert transform, often denoted $H(f)$, of a function $f(t)$ is defined as:

$$H(f)(t) = \frac{1}{\pi} \lim_{\epsilon \to 0} \int_{-\infty}^{\infty} \frac{f(t')}{t - t'} dt'. \tag{3.1}$$
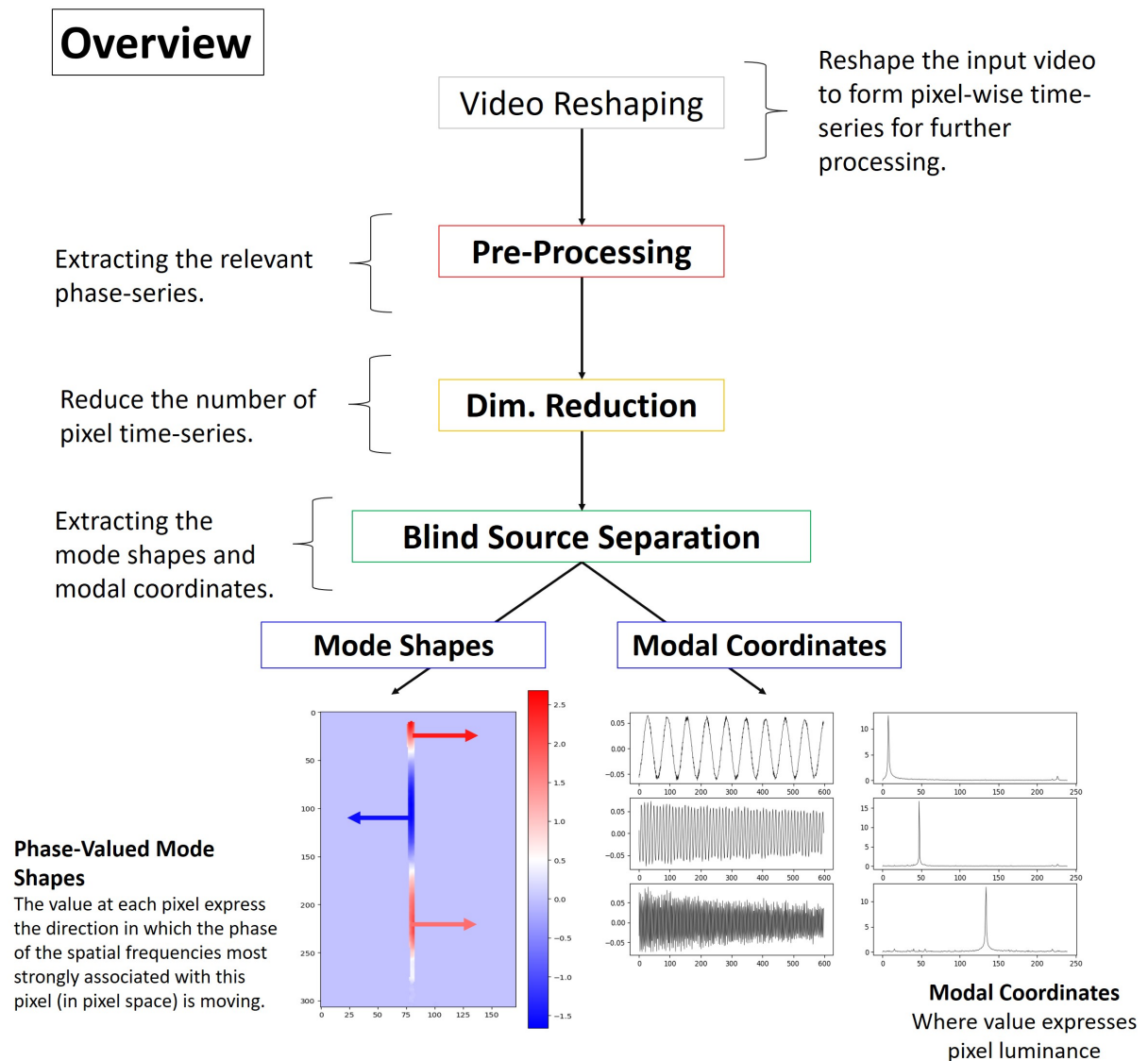
Figure 4 – Overview of the main steps involved in the framework for video-based structural dynamics estimation. Source: own elaboration.

Here, following the ideas proposed by [31] and [82], the role of the Hilbert transform for the task of estimating modal parameters from videos of vibrating structures is to extrapolate the phase-information, provided by the analytical signal, to augment the real-valued RGB data from the video to include phase as an additional information in the process of decomposition. Accessing the phase is crucial to detect spatial changes in the video. Common approaches make use of the phase-based optical flow [8] and Laplacian pyramids [83, 84] to take into account the spatial changes along with the temporal ones (raw-pixel values). However, as stated by Silva (2022) [31], the main advantage of the Hilbert-based approach over the aforementioned ones relies on the simplicity in terms of implementation and processing, allowing to simplify and speed-up the computational burden.
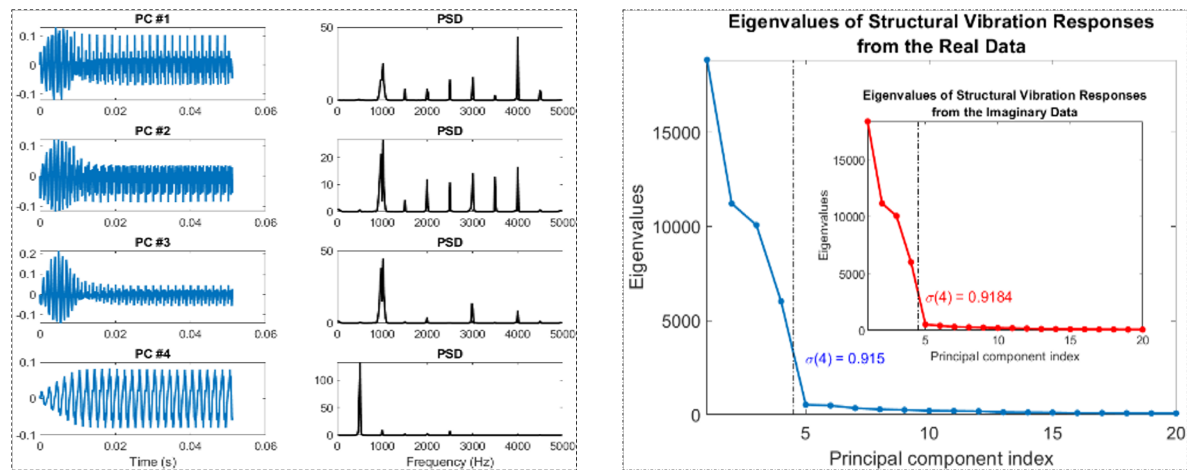
Figure 5 – Ilustration of the dimensionality reduction step. The ideia is to reduce the number of time series while retaining as much information as possible. Source: own elaboration.

## 3.2 Dimensionality Reduction for Modal Analysis

Dimensionality Reduction is a mandatory step for full field, high-resolution modal identification from video. After the pre-processing step, each pixel effectively becomes a measurement point and the number of time series is the resolution of the video and, often, only very few active pixels exists. For this reason, dimensionality reduction is suitable. The compressed pixel time-series representation still a mixture of structural modes, and then BSS is required for decoupling. Figure 5 ilustrates the DR step.

Two techniques are applied interchangeably: PCA and NNMF. Both are applied over all of the pixel time-series to perform a transformation from a high-dimensional space into a low-dimensional space. The low-dimensional space should retain the meaningful properties of the original data.

In order to perform DR of the data from video of vibrating structures, PCA is applied across all of the time series at each pixel (not frames). It is expected the principal components to be closely related to the modal components, although not exactly matching them . Ideally, the number of non-trivial eigenvalues calculated from the displacement time series is of the same order as the number of observable mode shapes. Therefore, the number of eigenvectors that correspond roughly to the number of nontrivial singular values is enough to retain the significant properties. Additionally, in this work, the PCA entry data was augmented by using Hilbert Transform to obtain both real and imaginary principal components.

For the dimensionality reduction of the data from video of vibrating structures problem, the entries of the NNMF algorithm are all the raw time-series from each pixel. It is assumed that the non-negative factors in **W**, provided by the temporal decomposition process, are related to the modal components by indicating the time pattern of a specific vibration mode. The matrix **H** incorporates a spatial decomposition and, when properly reshaped, resembles (but not exactly) the corresponding vibrational mode shapes.

## 3.2.1 Blind Source Separation for Modal Analysis

Using the dimension reduced components from PCA or NNMF, the BSS step assumes, in the case of video-based structural dynamics applications, the structural vibration measured into the recorded video frames as a local time-varying motion from a temporally translated image intensity $I(y + \delta(y, t))$, where $y$ is the pixel coordinate. The vibration motion is expressed in terms of a mixing mechanism, where $S$ is a set of individual source signals (individual motions), $s_i$ over time ($t$), weighted by some mixing component $A = [a_i]$ as

$$\delta(y, t) = \sum_{i=1}^{k} s_i(t)a_i = \mathbf{SA}, \tag{3.2}$$

where, $k$ is the number of vibration modes [12]. This is also expressed as a modal superposition, that is a liner combination of modal responses of an arbitrary structural system.

$$\delta(y, t) = \mathbf{q}(t)\Phi(y) = \sum_{i=1}^{k} q_i(t)\phi_i(y), \tag{3.3}$$

where $\mathbf{q}$ is the modal response matrix with $q_i(t)$ being the $i$-th modal coordinate, and $\Phi$ the mode shape matrix with each $\phi_i(y)$ as the $i$-th mode shape. In the end, it should be noted that the resulting BSS decomposition yields, directly, both the mode shapes and modal coordinates, with the later being the same as the sources estimated from the BSS. Other modal parameters, such as natural frequencies and damping ratios can be further estimated using conventional Fourier transform and logarithmic decrement techniques.

Several algorithms have been proposed in the literature to solve the BSS problem. Surrounded by a great number of BSS solutions, this work investigates six methods for video-based structural dynamics, namely: Complexity Pursuit (CP), Independent Component Analysis (ICA), Second Order Blind Identification (SOBI), SOBI Robust Ortogonalization (SOBIRO), Equivariant Robust ICA (ERICA), Algorithm for Multiple Unknown Signals Extraction (AMUSE). CP is already a well-know algorithm for non-contact vision-based modal analysis [12, 13, 31]. The other BSS algorithms are discussed in the literature of traditional modal identificantion [24, 25, 26, 29, 30], nevertheless they have not been addressed to the non-contact applications.

In order to extract mode shapes and coordinates using only the videos of vibrating structures, twelve full-field high-resolution modal identification algorithms were used by integrating PCA or NNMF to one of the six BSS techniques. The methods using principal component analysis are: PCA-CP, PCA-ICA, PCA-SOBI, PCA-SOBIRO, PCA-ERICA and PCA-AMUSE. The methods whose dimensionality reduction is based on the nonnegative matrix factorization are NNMF-CP, NNMF-ICA, NNMF-SOBI, NNMF-SOBIRO, NNMF-ERICA and NNMF-AMUSE. Figure 6 ilustrates the techniques used for each step of the proposed framework.

# 3.3  Comparison of modal properties

In order to compare modal properties, it is useful to consider natural frequencies, real mode shape vectors, modal masses, modal kinetic and strain energies. Also modal damping ratios and complex mode shapes cab be examined for evaluation of th system with complex modes of vibration [85]. Here, in this work, the natural frequencies and the mode shapes are the parameters used to compare the proposed methods.

It is plain to see that a analysis comparison only has meaning for matched modes. These are estimates of the same physical mode shape and their entries correspond one-for-one with their counterparts. This study consider four scenarios for modal comparison:

- The matched modes identified by the approches based of PCA-BSS performing EMA on a video of a cantilever beam;

- The matched modes identified by the approches based of NNMF-BSS performing EMA on a video of a cantilever beam;

- The matched modes identified by the approches based of PCA-BSS performing EMA on a video of a bench-scale model of a three-story building strucutre;

- The matched modes identified by the approches based of NNMF-BSS performing EMA on a video of a bench-scale model of a three-story building strucutre;

## 3.3.1  Modal Assurance Criterion

Modal Assurance Criterion (MAC) is one of the most popular tools for the quantitative comparison of modal comparison. It is a statistical indicator, just like ordinary coherence. This least squares based form of linear regression analysis yields an indicator that is most sensitive to the largest difference between comparative values and results in modal assurance criterion that is insensitive to small changes or small magnitudes [85, 86, 87].

In general, the MAC is calculated as the normalized scalar product of the two sets of vectors $\Phi_A$ and $\Phi_X$. The resulting scalars are arranged into the MAC matrix as the follow equation:

$$MAC_{(r,q)} = \frac{|(\Phi_A)_r{}^T(\Phi_X)_q{}^T|^2}{((\Phi_A)_r{}^T(\Phi_X)_r)((\Phi_A)_q{}^T(\Phi_X)_q)}, \tag{3.4}$$

where the form of coherence function can be recognized, indicating the casual relationship between $\Phi_A$ and $\Phi_X$.

A equivalent formulation, after the vector multiplication, is:

$$MAC_{(A,X)} = \frac{|\sum_{j=1}^{n}(\Phi_A)_j(\Phi_X)_j|}{(\sum_{j=1}^{n}(\Phi_A)_j{}^2)(\sum_{j=1}^{n}(\Phi_X)_j{}^2)}. \tag{3.5}$$

The MAC takes value between 0 (representing no consistent correspondence) and 1 (representing a consistent correspondence). Acording to Pastor (2012) [85], values larger than 0.9 indicate consistent correspondence whereas small values indicate poor resemblance of the two shapes. Moreover, the following motives are reasonable to the MAC takes values near zero:

- The system is non-stationary resulting from changes in the mass, stiffness and damping properties during testing;

- The system is non-linear;

- There is noise on the reference mode shape;

- The parameter extraction technique is invalid for the measured data set;

- The mode shapes are linearly independent. While the MAC is not a true orthogonality check since the mass or stiffness matrices have not been included in the calculation, it can be used as an approximation of an orthogonality check Obviously, if the first four reasons can be eliminated, the MAC can be interpreted in a similar way as an orthogonality calculation.

On the other hand, the MAC has a value near unity for the following reasons:

- The number of response degrees of freedom is insufficient to distinguish between independent mode shapes;

- The mode shapes are a result of unmeasured forces to the system;

- The mode shapes are primarily coherent noise;

- The mode shapes represent the same motion different only by a scalar;

Therefore, if the first three reasons can be eliminated, the MAC can be used to indicate consistence shapes thereby indicating the validity of the modal scale factor. The ideal MAC matrix is not a unit matrix because the modal vectors are not directly orthogonal but mass orthogonal. However, the MAC matrix indicates which individual modes from the two sets relate to the each other. If two vectors are switched in one set, then the largest entries of the MAC matrix are no more on the leading diagonal and it resembles a permutation matrix.

The MAC can only indicate consistency, not validity, so it is mainly used in pre-test mode pairing. The MAC is incapable of distinguishing between systematic errors and local discrepancies. It cannot identify whether the vectors are orthogonal or incomplete.

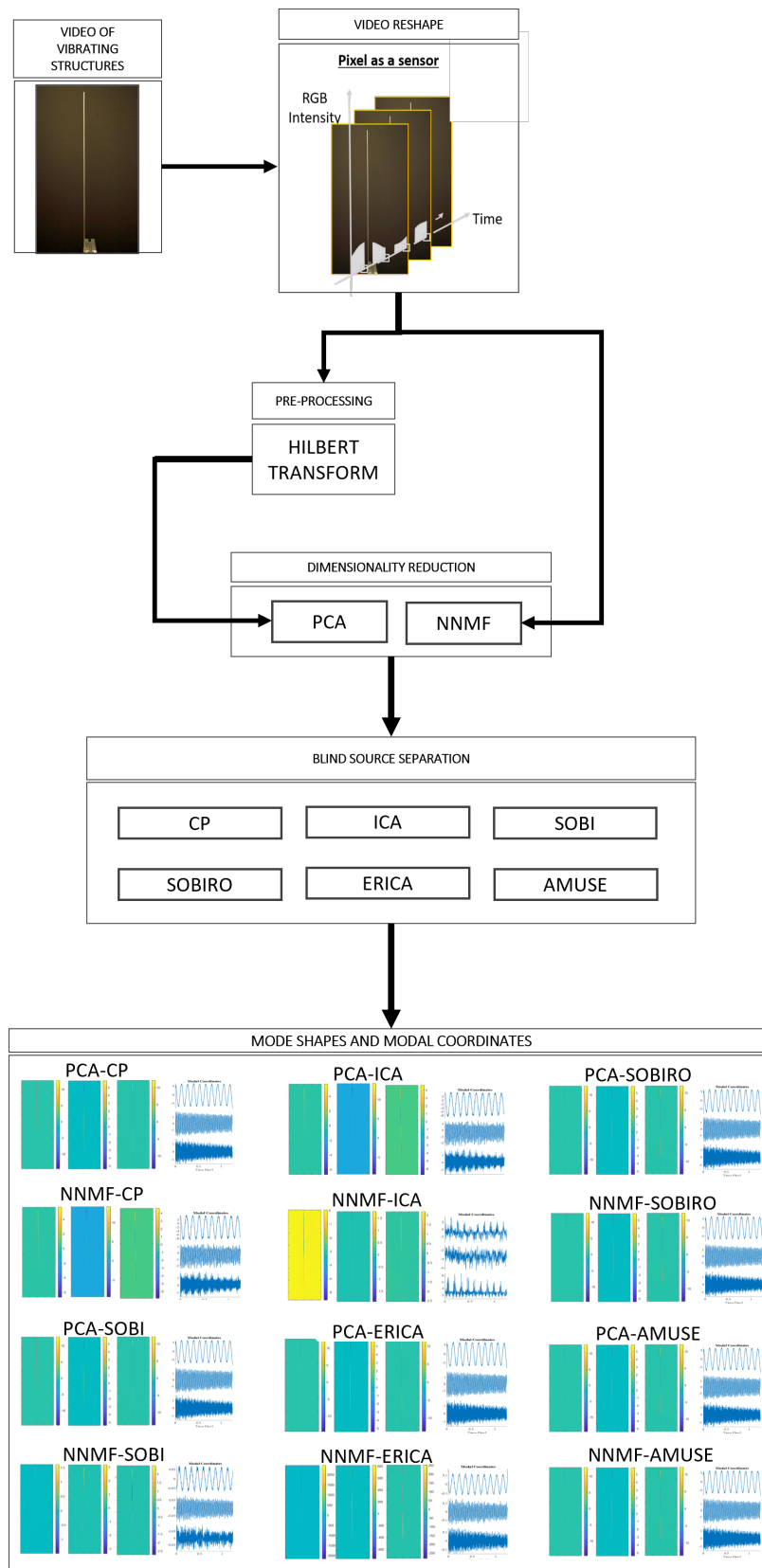Figure 6 – Overview of the methods proposed for video-based modal identification. First the video is reshaped and each pixel effectively becomes a measurement point. Then the HT is applied in each pixel time-series before PCA only. The DR step uses PCA and NNMF. They are combined with the six different BSS solution. A total of twelve algorithms are used to find the mode shapes and the modal coordinates. Source: own elaboration.

# 4  Results

The methods are validated from tests on a cantilever beam and a bench-scale building. Those are the same experimental setups studied by Silva(2020) [12] and they were chosen for the purpose of comparison. For the tests, a stationary camera (Sony NXCAM with a pixel resolution of 1920 × 1080) mounted by a Zeiss lens with a fixed focal length of 24 mm was used for video recording. The illumination environment was the ordinary indoor lighting condition without any external illumination enhancement. For comparisons, uniaxial accelerometers attached on the structures were used to measure the accelerations, from which the modal parameters were also extracted and compared with those estimated from the video measurement using the proposed methods.

## 4.1  Cantilever Beam

The modal identification algorithms were applied to an experimentally captured video of an aluminium cantilever beam. The structure was subjected to horizontal excitations close to the fixed end of the structure with an impact hammer (Figure 7). The stationary stationary camera previously described was used for video recording at a frame rate of 480 frames per second. The video is 216×384 pixels (a total of 82944 pixels) with 600 frames captured at 480 frames per second (a few frames are shown as grayscale images in Figure8). It is known from prior studies [8, 12] that the cantilever beam exhibits 3 modes. The measured natural frequencies of these modes are 7.2 Hz, 47.2 Hz and 133.6 Hz, which are consistent with those identified from accelerations of the beam.

### 4.1.1  Experimental Results

The twelve BSS-based methods attempt to identify the three vibration modes from the cantilever beam, along with their corresponding natural frequencies 7.2 Hz, 47.2 Hz and 133.6 Hz. Figures 9 to 14 give an outline of the PCA-based and NNMF-based approaches results. The figures show the modes shapes, the modal coordinates and their power spectral density (PSD). Figure 15 and 16 present the MAC comparing the six techniques for PCA and NNMF-based approach, respectively.

From the evaluation of the mode shapes and modal coordinates, as well the natural frequencies showed by the PSDs (Figures 9, 10 and 11), it is noticeable that for the PCA-based approaches, PCA-CP, PCA-ICA, PCA-SOBIRO and PCA-ERICA identified all three modal frequencies. On the other hand, PCA-SOBI was not able to identify the third mode shape, with the natural frequency equivalent to 133Hz.

PCA-AMUSE was not able to properly identify any of the three modes. In general, the first
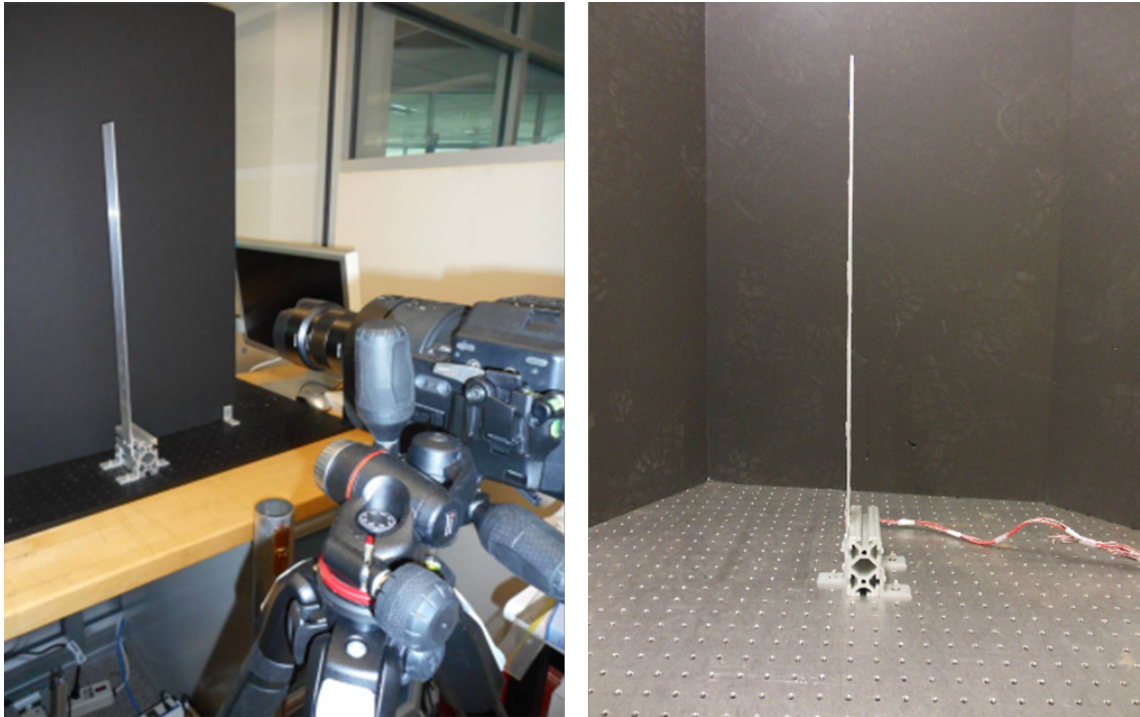
Figure 7 – The experimental cantilever beam setup. From Silva(2020) [12].



Figure 8 – A few temporal frames from the video measurement of the cantilever beam structure subjected to horizontal excitations.

five methods seem to agree well on the natural frequency estimates of the three modes. The MAC's for each mode between the six techniques are shown graphically in Figure 15 and supports the results.

PCA-CP, PCA-ICA, PCA-SOBI, PCA-SOBIRO and PCA-ERICA presented monotone modal coordinates using the first eight principal components. PCA-AMUSE, on the other hand, used 22 principal components to present modal coordinates with monotone behavior (often, a properly estimated mode is presented as a monotone signal). Since the number of modes to be estimated from the video is three, and ideally, when using PCA along with the Hilbert transform for data augmentation, the minimum number of principal components is twice the number of modes possible to verify into the measurements. However, here, we observe that none of the techniques worked properly when

Figure 9 – Mode shapes, mode coordinates and PSD obtained applying PCA-CP and PCA-ICA on the video measurement of the cantilever beam structure.



Figure 10 – Mode shapes, mode coordinates and PSD obtained applying PCA-SOBI and PCA-SOBIRO on the video measurement of the cantilever beam structure.

Figure 11 – Mode shapes, mode coordinates and PSD obtained applying PCA-ERICA and PCA-AMUSE on the video measurement of the cantilever beam structure.



Figure 12 – Mode shapes, mode coordinates and PSD obtained applying NNMF-CP and NNMF-ICA on the video measurement of the cantilever beam structure.

Figure 13 – Mode shapes, mode coordinates and PSD obtained applying NNMF-SOBI and NNMF-SOBIRO on the video measurement of the cantilever beam structure.
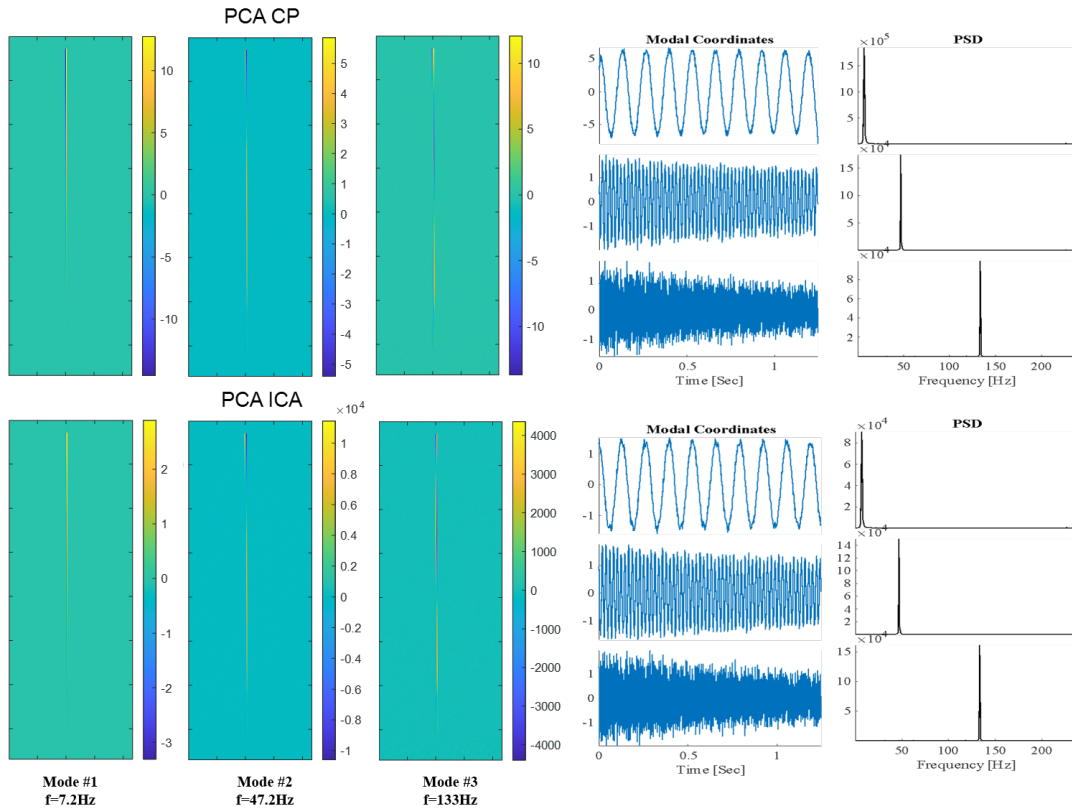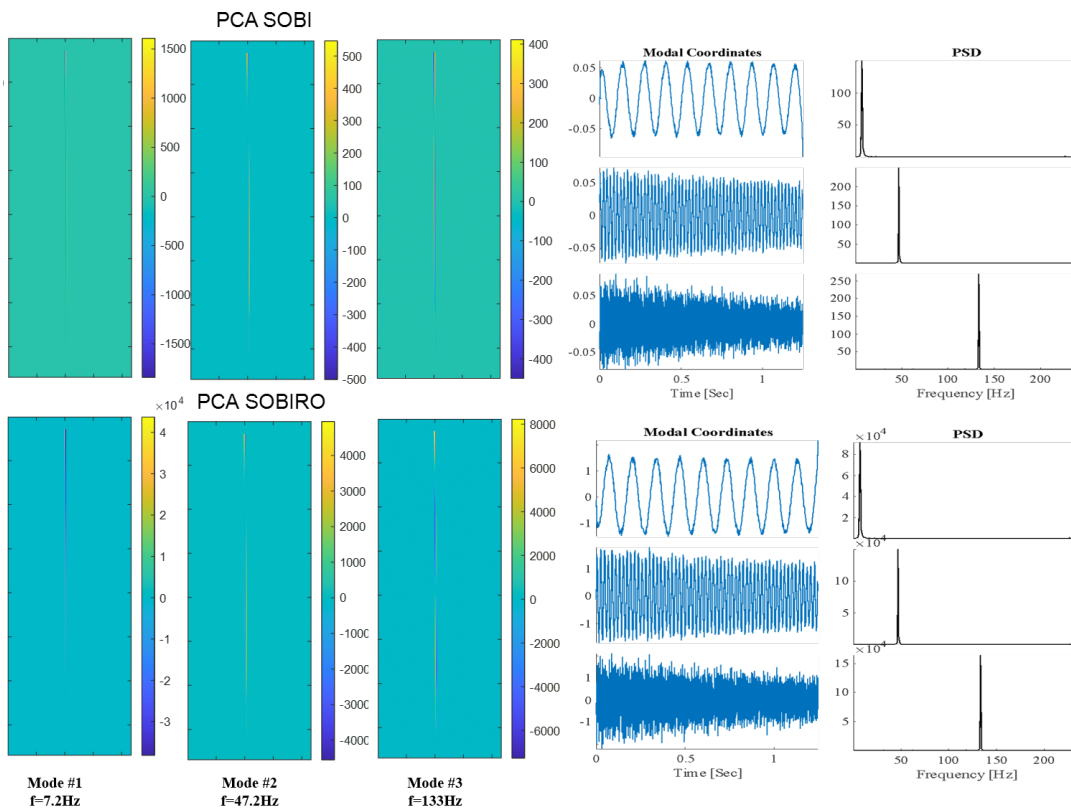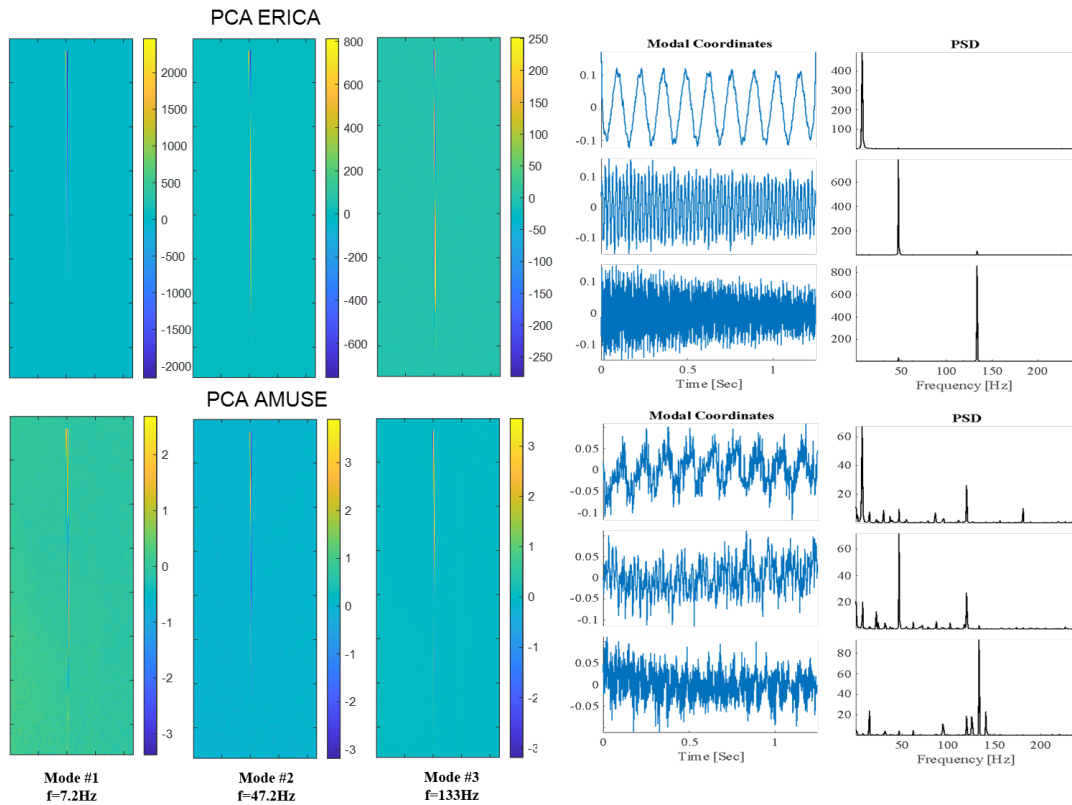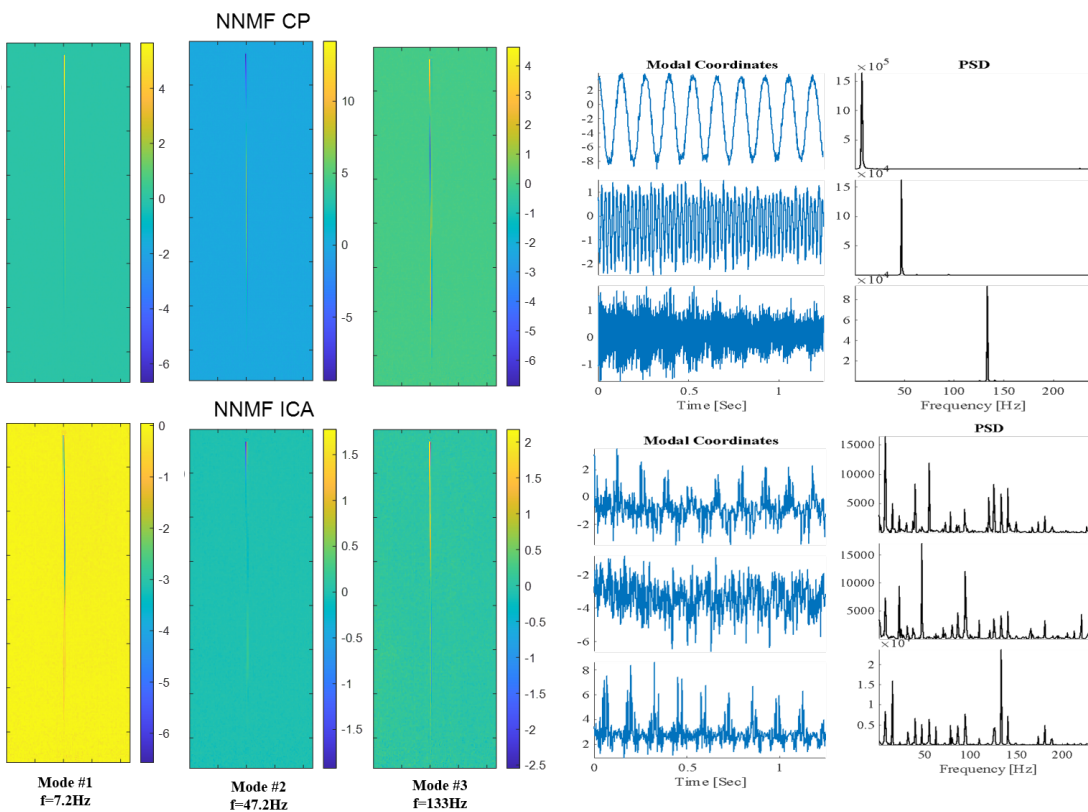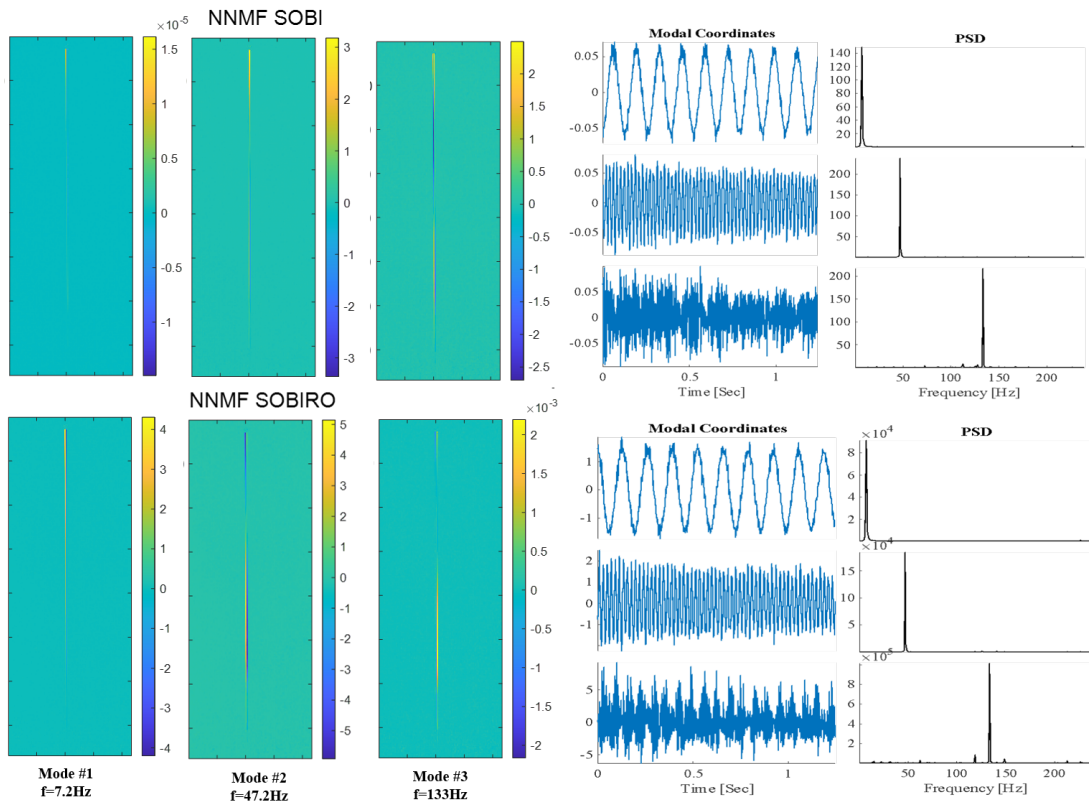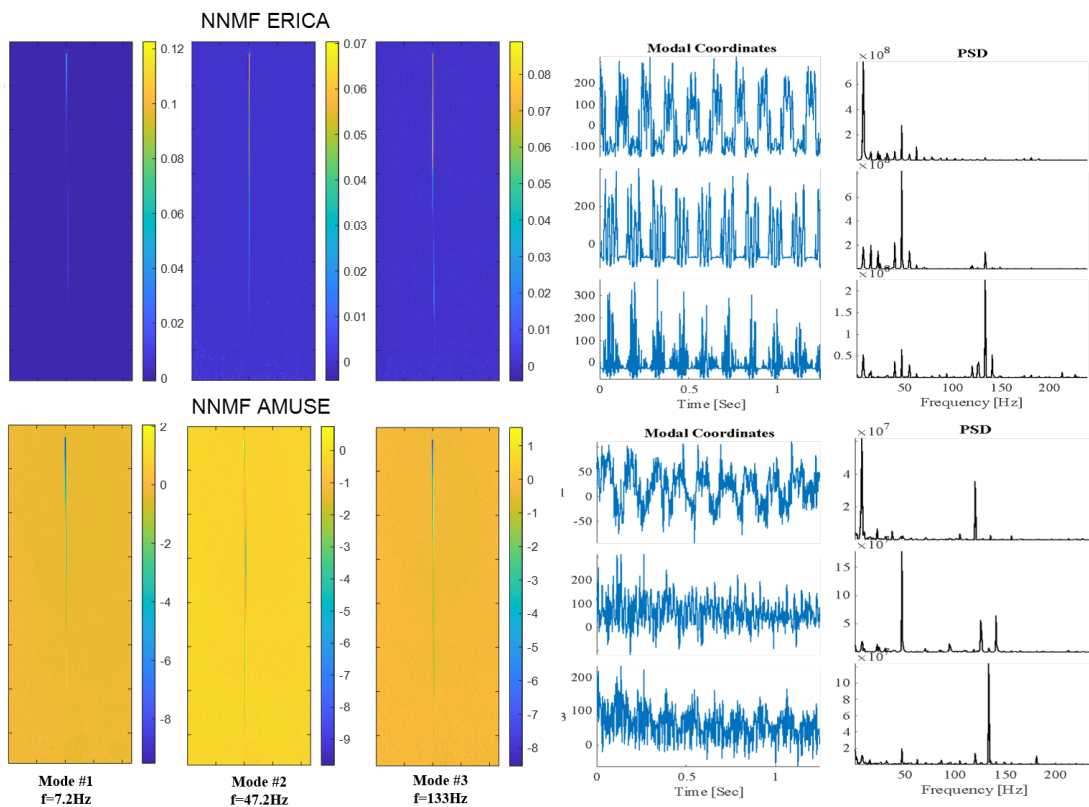


Figure 14 – Mode shapes, mode coordinates and PSD obtained applying NNMF-ERICA and NNMF-AMUSE on the video measurement of the cantilever beam structure.

Figure 15 – Modal Assurance Criterion (MAC): Measurement of the correlation of the vibration shapes obtained from PCA-based methods on the video of the cantilever beam.



Figure 16 – Modal Assurance Criterion (MAC): Measurement of the correlation of the vibration shapes obtained from NNMF-based methods on the video of the cantilever beam.

using six principal components, instead, eight components were required for most techniques.

In summary, among the PCA-based methods, the most consistent for identifying the three modes are PCA-CP, PCA-ICA, PCA-SOBIRO and PCA-ERICA, although the third mode for the last method does not totally agree with the modes estimated using the other methods. PCA-SOBI and PCA-AMUSE are not indicated for the task of performing dynamics identification from video measurements, as they were not capable to estimate the three modes. More specifically, PCA-AMUSE could not estimate any of the modes, at any level; on the other hand, PCA-SOBI performed well on identifying the first two modes, but was not able to find the third mode.

Also from the evaluation of the mode shapes and modal coordinates and PSDs, for the NNMF-based methods, the NNMF-CP was the most successful in identifying the three mode frequencies properly. The first and second modes were identified by NNMF-CP, NNMF-SOBI and NNMF-SOBIRO. NNMF-ICA, NNMF-ERICA and NNMF-AMUSE were not able to properly identify the vibration modes.

NNMF-AMUSE was not successful in estimating any of the three modes, confirming its poor performance in performing modal analysis in the context of a video-based framework. For the remaining methods, NNMF-ICA and NNMF-ERICA also performed poorly when attempting to estimate any of the modes. Although PCA-SOBIRO was able to reasonably estimate the first two modes, it found problems for estimating the third one, mainly when considering the mode shapes. In general, when using NNMF as the dimensionality reduction technique, only CP and SOBI demonstrated to

derive reasonable and consistent results in terms of mode shape estimation.

NNMF-CP, NNMF-SOBI and NNMF-SOBIRO presented monotone modal coordinates using the first ten nonnegative factors from NNMF. On the other hand, PCA-ERICA used 15 factors. PCA-ICA and PCA-AMUSE used 20 components to present modal coordinates with monotone behavior.
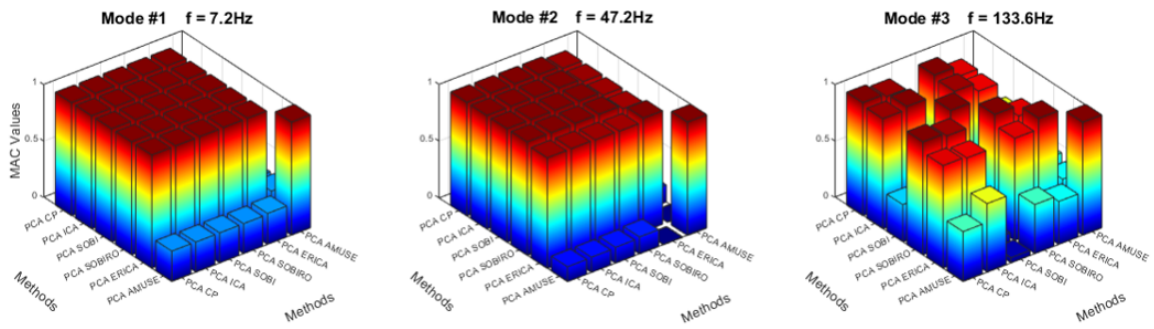
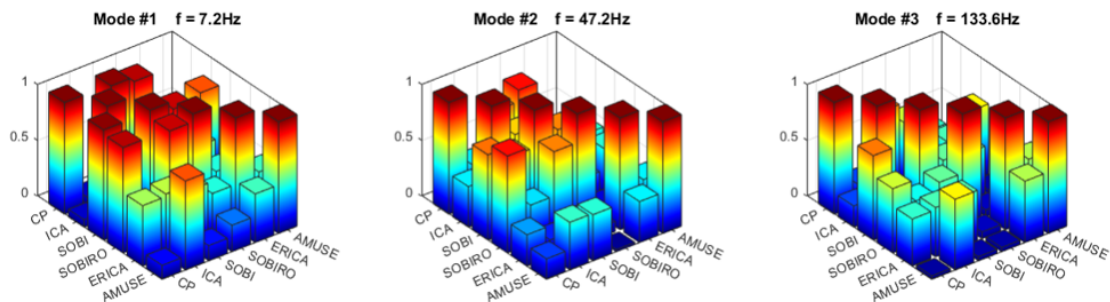Figure 15, which shows the measurement of the correlation of the vibration shapes obtained from PCA- based methods on the video of the cantilever beam, indicates which individual modes from the two sets relate to the each other. For the first and second modes, characterized by the natural frequency 7.2 Hz and 47.2 Hz respectively, the only method taking on values near zero is PCA-AMUSE, which only agrees with its own result. PCA-CP, PCA-ICA, PCA-SOBI, PCA-SOBIRO and PCA-ERICA quantify values larger than 0.9 (compared to each other), indicating consistent correspondence among them for the video of the cantilever beam.

The MAC of the third mode (133.6 Hz) shows that the values comparing PCA-CP, PCA-ICA and PCA-SOBIRO are larger than 0.9. PCA-ERICA quantifies the same value, 0.86. These results indicates the mentioned four methods present a consistent correspondence. In this manner, the modal vectors under consideration truly exhibit a expected linear relationship. PCA-SOBI, compared to the other five methods, takes on values near 0.3 and PCA-AMUSE is evaluated between zero (compared to PCA-SOBI) and 0.7 (compared to PCA-ICA). This is an indication that the modal vectors are not consistent for both methods. These results are, in fact, validated by the analysis of the mode shapes and modal coordinates.

The measurements of the correlations of the vibration shapes obtained from NNMF-based methods on the video of the cantilever beam are described by the Figure 16. For the first mode (7.2 Hz); NNMF-CP, NNMF-SOBI and NNMF-SOBIRO have a consistent correspondence relating to each other, represented by values near the unity. NNMF-ICA has no correspondece to NNMF-CP and NNMF-SOBI, with values near to zero compared to them. However, NNMF-ICA has some correspondence to NNMF-ICA (near 0.8) and NNMF-ERICA (0.6). NNMF-ERICA also was evaluated near 0.6 compared to the other methods. The qualitative analysis shows that, although NNMF-ICA, NNMF-ERICA and NNMF-AMUSE have correspondece to each other, their modal coordinates do not present a monotone behavior

The MAC of the second mode (47.2 Hz) shows that NNMF-CP agrees to NNMF-SOBIRO (0.9) and NNMF-SOBI (0.88), althoug the MAC values is not greater than 0.9, they are near to each other. NNMF-SOBIRO's second mode correspond to NNMF-SOBI(0.86). NNMF-ICA, NNMF-ERICA and NNMF-AMUSE have no consistent correspondence copared to any other method. In fact, although the MAC values between NNMF-ICA and NNMF-AMUSE, NNMF-SOBI and NNMF-AMUSE and NNMF-ERICA and NNMF-AMUSE are not near to zero, they are small and can be considered consistent.

Comparing the NNMF-based methods to identify mode 3, with the natural frequency equiv-

alent to 133.6 Hz, the MAC shows which pairs of methods are correlated. The pairs NNMF-CP with NNMF-ICA and NNMF-CP with NNMF-AMUSE have MAC values near to zero, i.e., they are not related. NNMF-CP correspont to NNMF-SOBI with the MAC value 0.8. NNMF-CP also has shown some correspondece to NNMF-SOBIRO (0.65) and a really small correspondece to NNMF-ERICA (less than 0.5). NNMF-ICA and NNMF-AMUSE correspond to each other with a MAC value 0.7. NNMF-ERICA results also has a small correspondence to the ones accomplished by NNMF-ICA and NNMF-AMUSE.

In general, for the present case, the BSS algorithms integrated into PCA presented better modal identification performance than the NNMF-based methods. It is found that CP properly performed modal analysis combined with both dimensionality reduction methods. ICA and ERICA only identified the modal shapes and mode coordinates combined with PCA. Coupled with PCA, SOBI adequately identified the first two modes only, demonstrating a better performance when used along with the NNMF as it identified all modes. Regarding the SOBIRO-based method, it identified the three modes with PCA and only the first two modes combined with NNMF. AMUSE was not successful in accomplishing full-field high-resolution modal identification from the video of the cantilever beam structure in any case.

## 4.2 Bench-scale building

As showed in Figure 17, a bench-scale model of a three-story building structure was also used to validate the proposed approaches. The structure consists of aluminum columns and lumped mass plates on each floor, with its base fixed to a heavy solid aluminum plate on the ground. In this scenario, an impact hammer was used to excite the structure horizontally on the top floor. The stationary camera was used to perform video measurements of the structure at a frame rate of 240 frames per second. a few frames are shown in Figure 18 It is known from prior analysis that the cantilever beam exhibits 3 modes. The measured natural frequencies of these modes are 6.3 Hz, 18 Hz, and 25 Hz.

### 4.2.1 Experimental Results

The twelve BSS-based methods attempt to identify the three vibration modes from model of a three-story building structure, along with their corresponding natural frequencies 6.3 Hz, 18 Hz, and 25 Hz. Figures 20 to 21 give an outline of the PCA-based results and Figures 22 to 24 show the NNMF-based approaches results. The figures show the modes shapes, the modal coordinates and their PSD. Figure 25 and 26 present the MAC comparing the six techniques for PCA and NNMF-based approach, respectively.

From the qualitative analysis from the mode shapes and modal coordinates, the methods seem to agree well on the natural frequency estimates of the three modes. PCA-CP (Figure 19), PCA-SOBI, PCA-SOBIRO (20) and PCA-ERICA (Figure 21) identified all three modal frequencies. On the other hand, PCA-ICA was not able to identify any mode properly. Using ICA, it is possible to observe
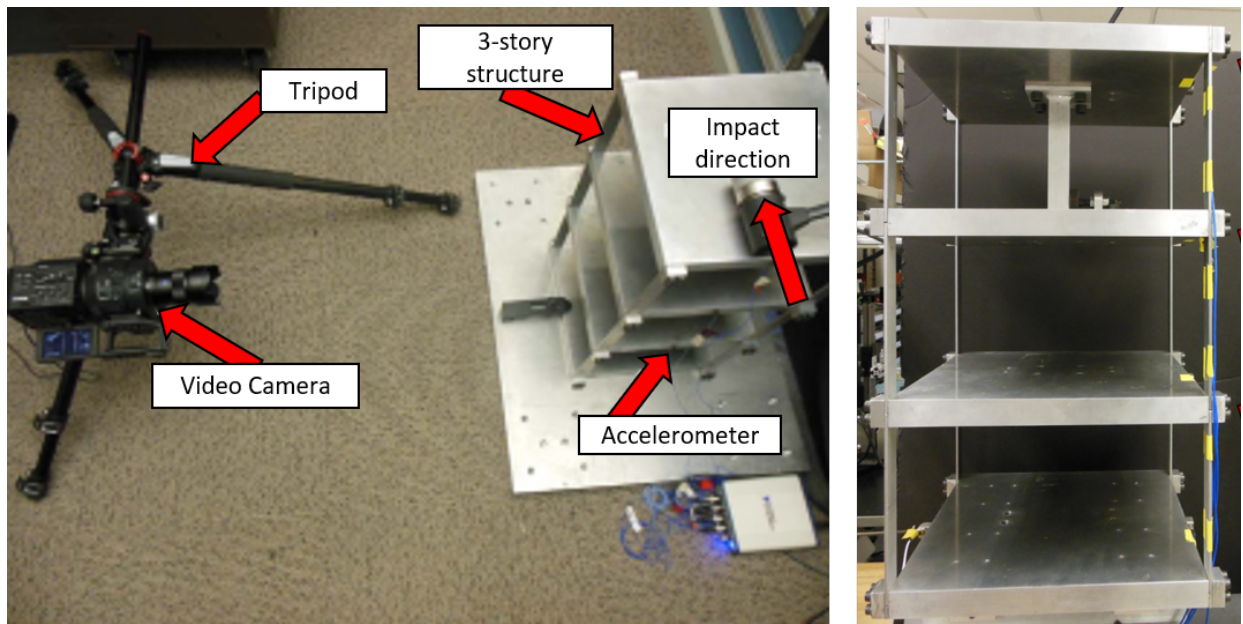
Figure 17 – Three-story frame aluminum structure setup. From Silva(2020) [12].
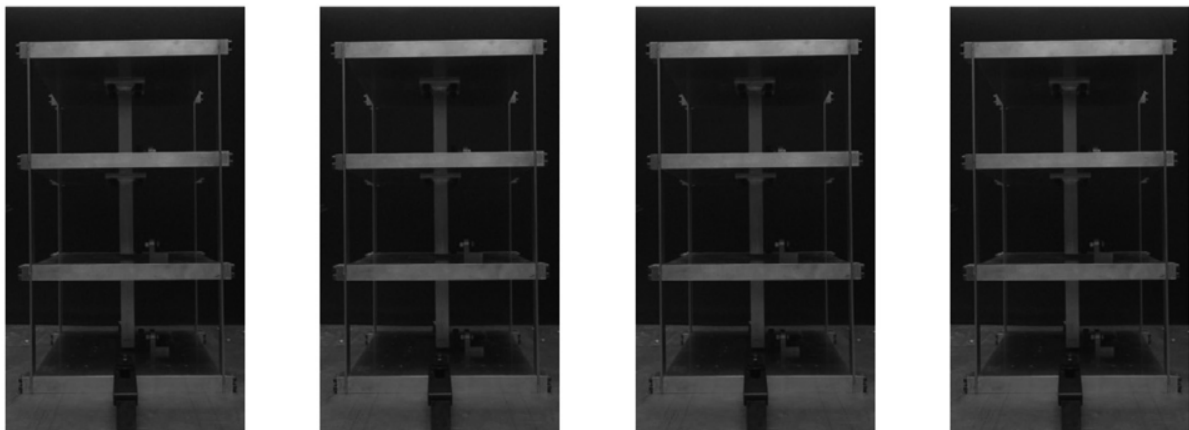


Figure 18 – A few temporal frames from the video measurement of the three-story building structure subjected to horizontal excitations.

interference from other frequencies in all modes, albeit small. PCA-AMUSE only identified correctly the first mode.

Regarding to the number of principal components used to perform PCA, the method PCA-SOBIRO presented monotone modal coordinates using the first 14 principal components; while PCA-SOBI and PCA-ERICA used principal 16 principal components; PCA-CP, PCA-AMUSE and PCA-ICA used 22, 26 and 28 components to present modal coordinates with monotone behavior, respectively. It is interesting to point out that, in general, to perform the dynamic analysis of the bench-scale model of a three-story building structure, all the methods required more principal components comparing to the cantilever beam problem.

PCA-based methods, the most consistent for identifying the three modes are PCA-CP, PCA-SOBI, PCA-SOBIRO and PCA-ERICA. PCA-ICA and PCA-AMUSE are not indicated for the task of performing dynamics identification from video measurements in this problem specifically, as they
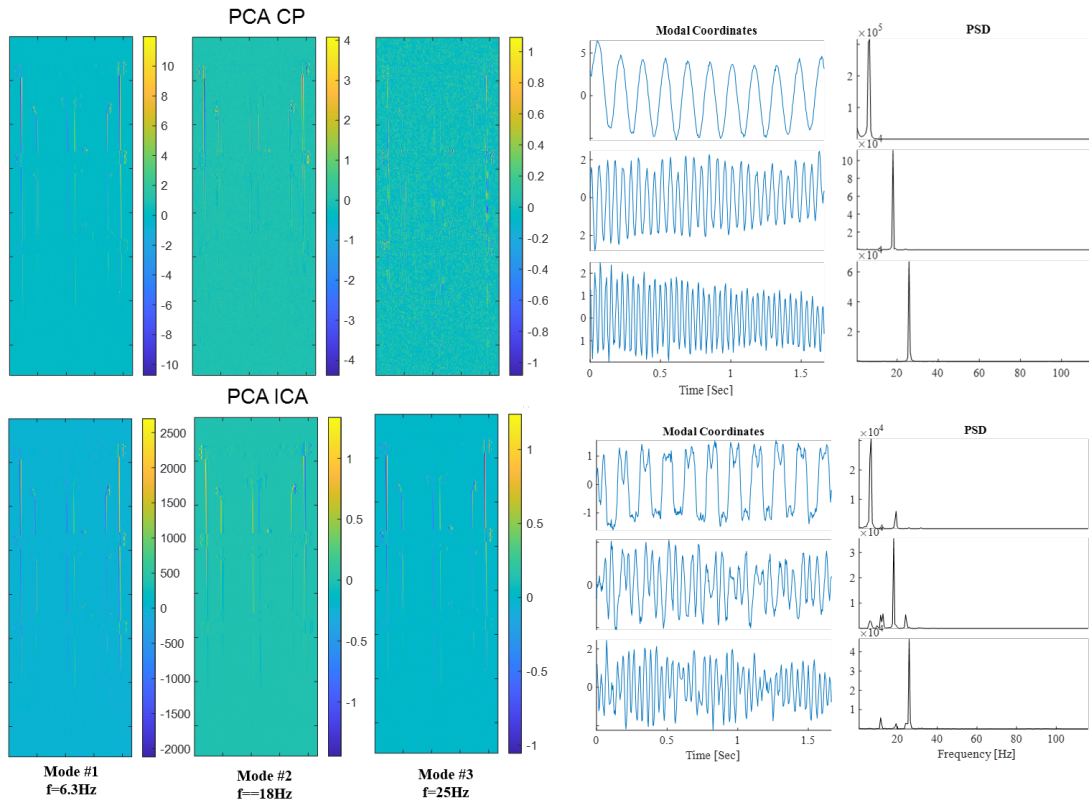
Figure 19 – Mode shapes, mode coordinates and PSD obtained applying PCA-CP and PCA-ICA on the video measurement of the three-story building structure.
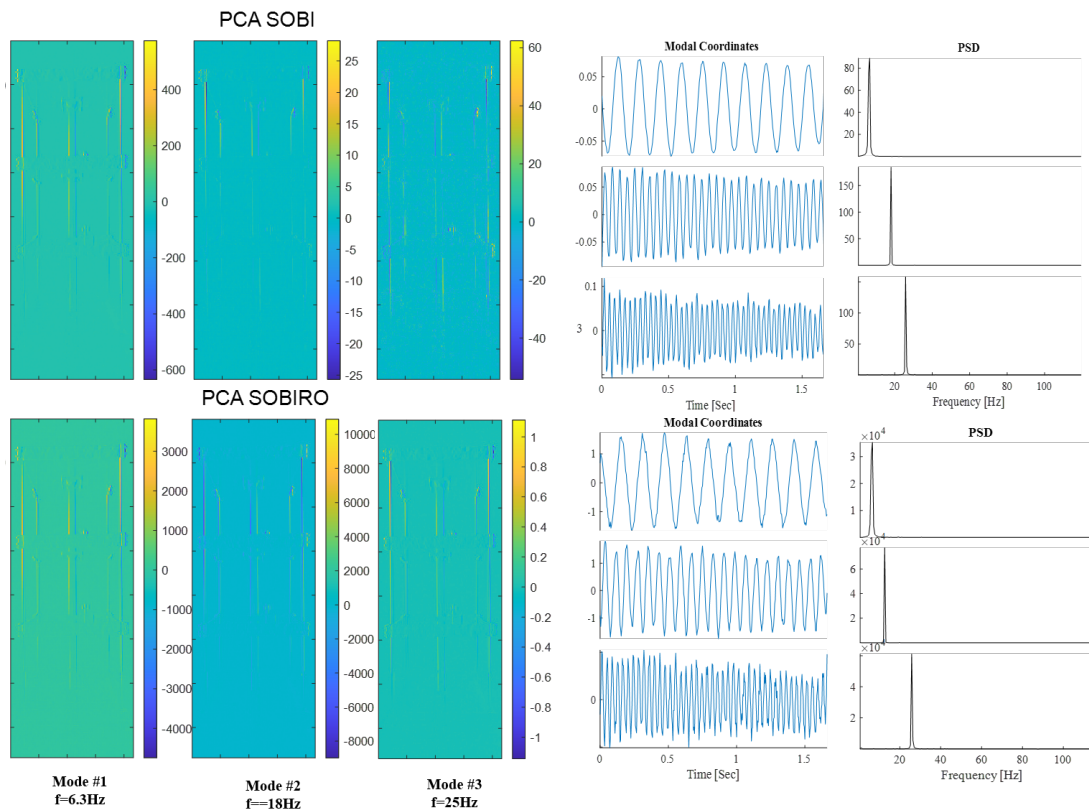


Figure 20 – Mode shapes, mode coordinates and PSD obtained applying PCA-SOBI and PCA-SOBIRO on the video measurement of the three-story building structure.
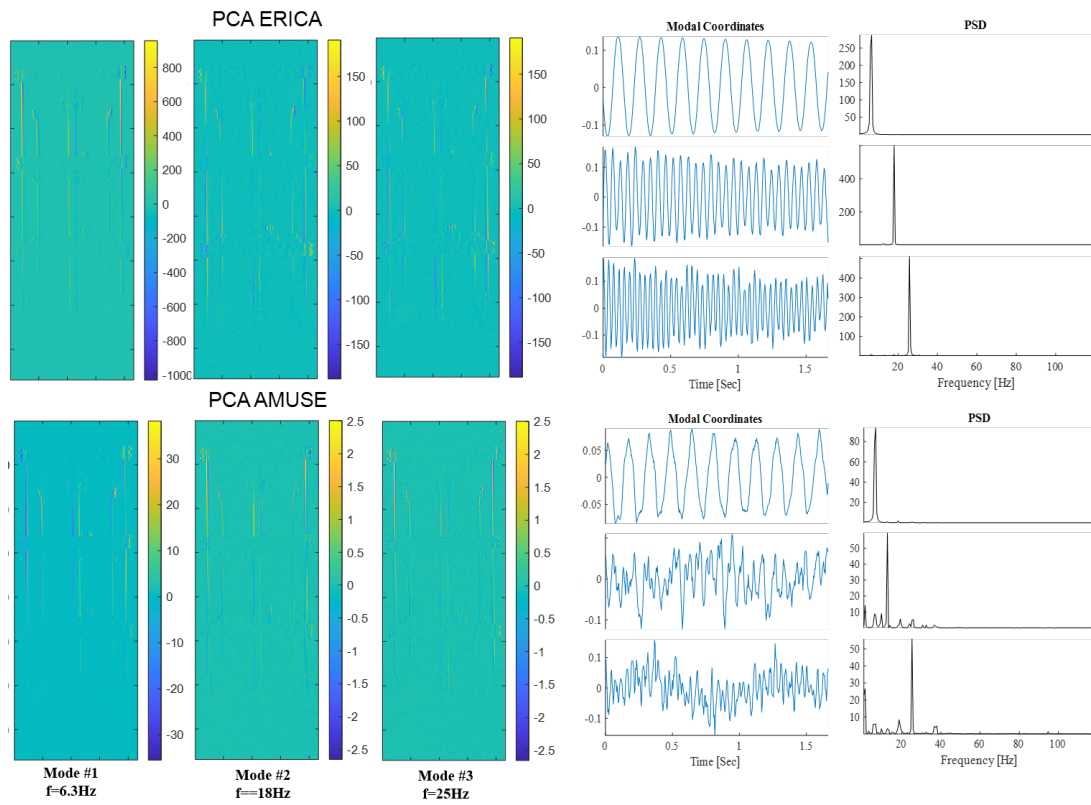
Figure 21 – Mode shapes, mode coordinates and PSD obtained applying PCA-ERICA and PCA-AMUSE on the video measurement of the three-story building structure.
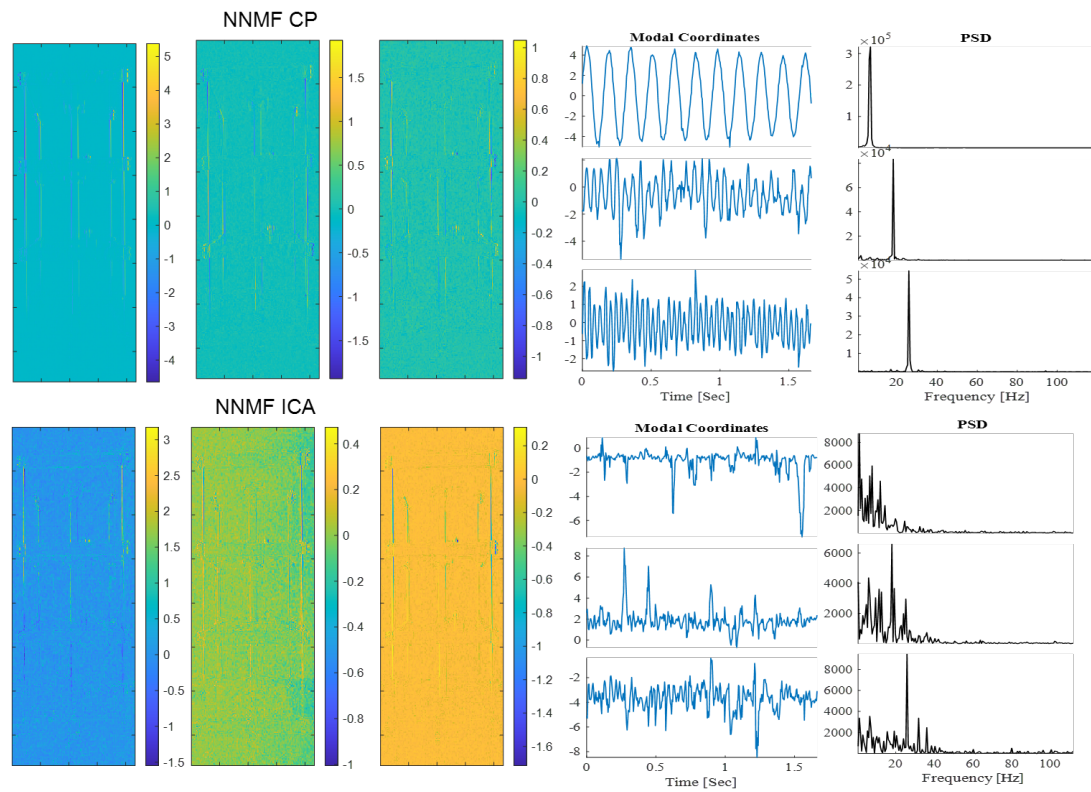


Figure 22 – Mode shapes, mode coordinates and PSD obtained applying NNMF-CP and NNMF-ICA on the video measurement of the three-story building structure.
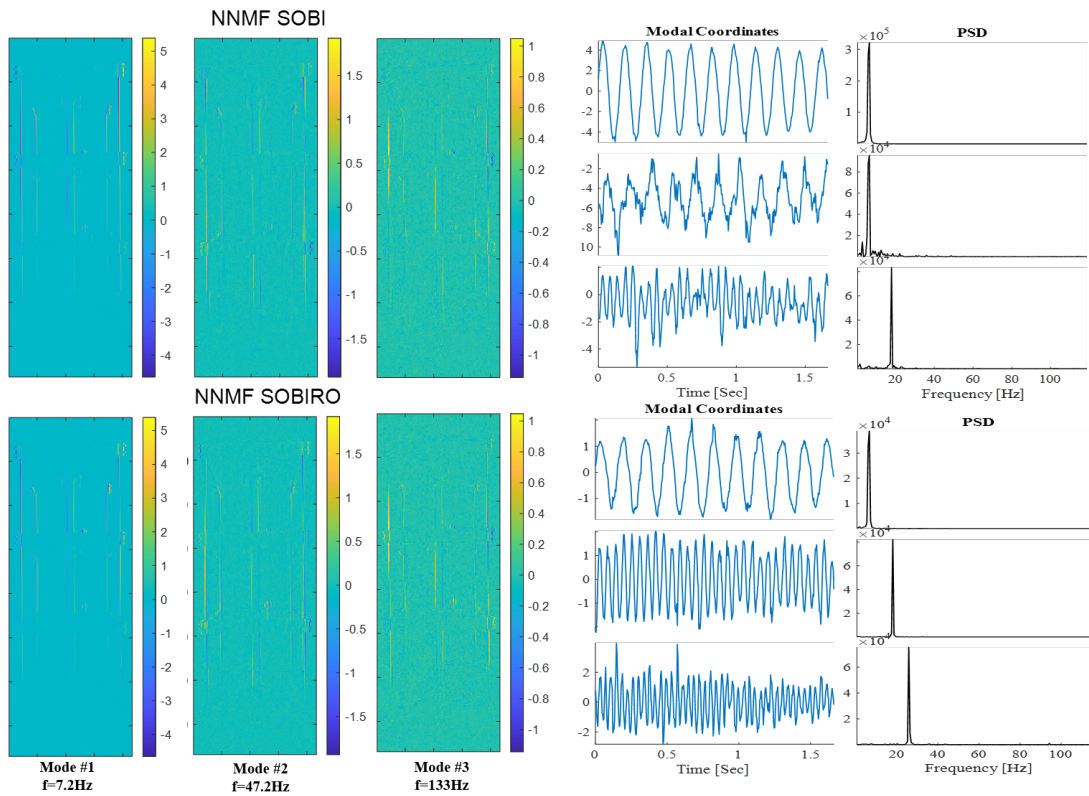
Figure 23 – Mode shapes, mode coordinates and PSD obtained applying NNMF-SOBI and NNMF-SOBIRO on the video measurement of the three-story building structure.
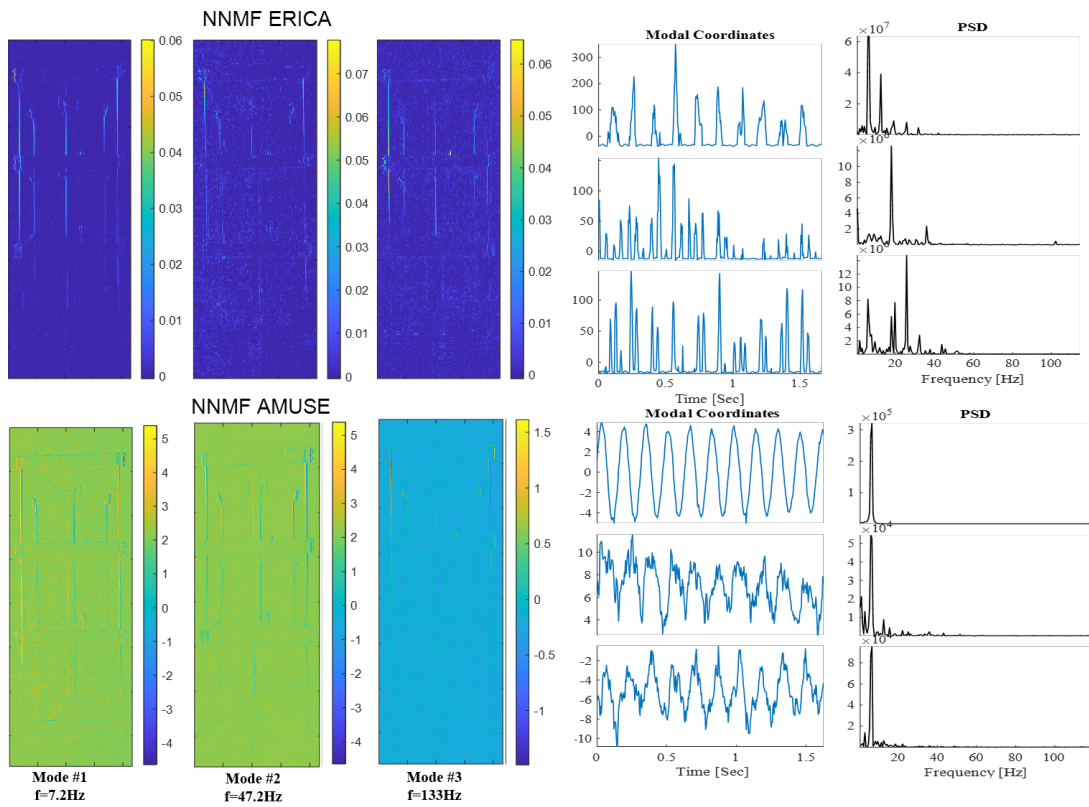


Figure 24 – Mode shapes, mode coordinates and PSD obtained applying NNMF-ERICA and NNMF-AMUSE on the video measurement of the three-story building structure.
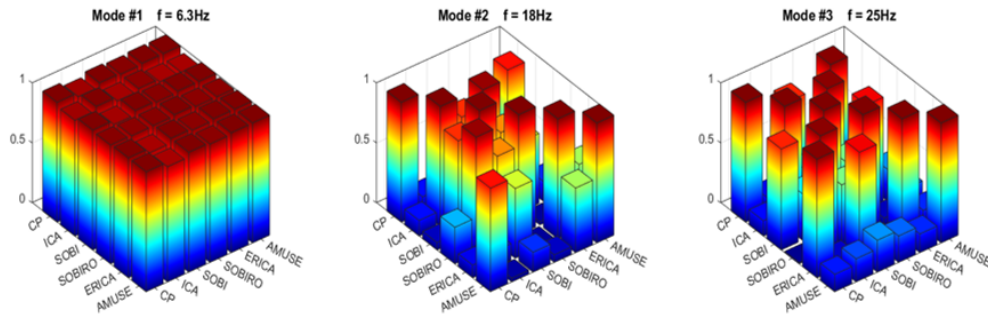
Figure 25 – Modal Assurance Criterion (MAC): Measure of the correlation of the vibration shapes obtained from PCA-based methods on the video of the three-story building structure.
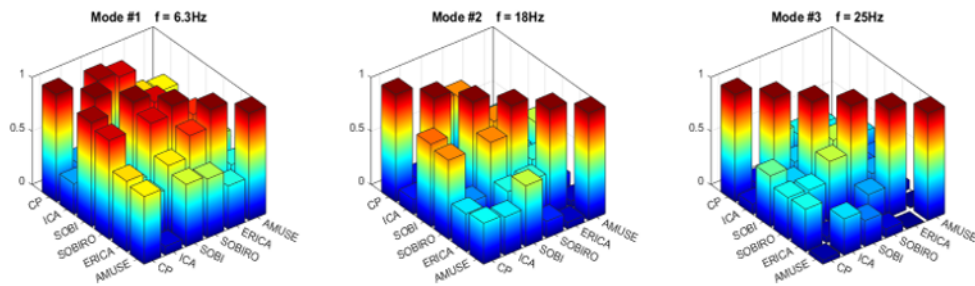


Figure 26 – Modal Assurance Criterion (MAC): Measure of the correlation of the vibration shapes obtained from NNMF-based methods on the video of the three-story building structure.

were not capable to estimate the three modes. PCA-ICA did not estimate any of the modes clearly; PCA-AMUSE performed well on identifying the first mode, but was not able to find the second and the third ones.

With reference to NNMF-based methods, NNMF-CP, NNMF-SOBI and NNMF-SOBIRO (Figures 22 and 23) were successful in identifying the three modal frequencies properly. NNMF-ERICA and NNMF-AMUSE (Figure 24) seems to discern the natural frequencies of the system, however, all three modes show the presence of other frequencies (perceptible on the PSD). NNMF-ICA, in turn, could not identfy any of the modes, at any level.

To perform the modal analysis of the three-story building structure NNMF-CP and NNMF-SOBIRO used 22 components. NNMF-ICA, NNMF-ERICA, NMMF-AMUSE used 28 components each. NNMF-SOBI used 32.

Measurements of the correlation between the vibration shapes obtained from PCA-based methods on the video of the bench-scale building, showed in the Figure 25,indicates which individual modes from the two sets relate to the each other. For the first mode, characterized by the natural frequency 6.3 Hz, all the methods presetend a consistent corresponce to each other, all MAC values are greater than 0.9.

The MAC values of the second mode (with the natural frequency of 18 Hz) shows that the values PCA-CP only has correspondece greater than 0.9 to PCA-AMUSE. Even though, PCA-ICA

does not correspond to PCA-CP, it corresponds to PCA-SOBI (0.85) and PCA-SOBIRO (near the unity). PCA-SOBI also has some correspondece, with MAC value 0.72 and 0.85 respectivaly, with PCA-ERICA and PCA-SOBIRO. These results indicates that, regardless of the non generalized correspond (as in the first mode), the modes identified by the methods can be considered correlated.

With the natural frequency 25 Hz, the third mode indentified by PCA-CP has a MAC value near 0.9 paired to PCA-SOBI and PCA-ERICA. The last one also has a consistent correspondence with the mode indentified by NNMF-SOBI. NNMF-ICA only correlates consistently (0.9) with NNMF-SOBIRO. The mode identified by NNMF-AMUSE is not correlated to any other method, all the MAC values are less than 0.4.

Correlations of the vibration shapes obtained from NNMF-based methods on the video of the three-story bulding structure are described by the Figure 26. Concerning to the identification of the first mode; NNMF-CP, NNMF-SOBI and NNMF-SOBIRO have a consistent correspondence relating to each other, represented by values near the unity. NNMF-CP also is correlated by a factor near 0.7 with NNMF-ERICA and NNMF-AMUSE. NNMF-ICA result does not correspond to any othe result. NNMF-SOBI also agrees (near 0.7 of MAC values) to NNMF-AMUSE and NNMF-ERICA; it also has a consistent correspondece, near 0.9, with NNMF-SOBIRO. The mode identified by NNMF-SOBIRO is also related to NNMF-ERICA (0.85). NNMF-AMUSE has a MAC value greater than 0.6 compared to NNMF-CP, NNMF-SOBI and NNMF-SOBIRO, i.e., they are have a correlation.

The MAC of the second mode ($f = 18$ Hz) shows that NNMF-CP agrees to NNMF-SOBI and NNMF-SOBIRO by a MAC factor near 0.8. The other relevant correspondence for this mode is between the pairs NNMF-SOBI/NNMF-SOBIRO and NNMF-SOBI/NNMF-AMUSE, near 0.8. For the identification of the mode number three, with $f = 25$ Hz, the only relevant correlations due to MAC values greater than 0.6 are NNMF-CP with NNMF-SOBI and NNMF-SOBI with NNMF-SOBIRO.

It is important to state that MAC measures the degree of linearity (consistency) between two modal vectors. However, to the authors' knowledge, the modal assurance criterion can only indicate consistency, not validity or orthogonality. If the same errors, random or bias, exist in all modal vector estimates, this is not delineated by the criterion.

In general, for that case, both dimensionality reduction methods, PCA and NNMF, performed modal identification satisfactorily. Combined to the BSS tecniques, it is found that CP, SOBI and SOBIRO properly performed modal analysis combined with both dimensionality reduction methods. ICA and AMUSE did not identified the modal shapes and mode coordinates combined with any of them. Coupled with PCA, ERICA adequately identified the three modes, while when used along with the NNMF it was not suitble at all.

## 4.3   Summary and Discussion

Table 2 shows a brief summary of the applied methods for modal analysis on the cantilever beam problem. In general, the ones based on PCA to perform the dimensionality reduction presented a slightly better response in terms of the number of components and number of identified modes. Among the twelve proposed methods, eight were capable to fully indentify the three modes. That is possible to notice that ICA works well when combined to PCA, but it was not a good technique when combined to NNMF. NNMF and SOBI were a better combination than PCA and SOBI.

| Dimensionality Reduction | Blind Source Separation | #Components | Number of Modes |
|---|---|---|---|
| PCA | CP | 8 | 3 |
| | ICA | 8 | 3 |
| | SOBI | 8 | 2 |
| | SOBIRO | 8 | 3 |
| | ERICA | 8 | 3 |
| | AMUSE | 22 | 0 |
| NNMF | CP | 10 | 3 |
| | ICA | 20 | 0 |
| | SOBI | 10 | 3 |
| | SOBIRO | 10 | 3 |
| | ERICA | 8 | 3 |
| | AMUSE | 22 | 0 |

Table 2 – Summary of the results of the vibration response from the cantilever beam structure.

Table 3 shows a brief summary of the applied methods for modal analysis on bench-scale building structure problem. Four of the six PCA-based methods were able to fully identify the three modes. ICA, as in the first problem, showed to be not appropriate to perform modal analysis. ERICA did not work combined to NNMF. AMUSE did not work at any level.

| Dimensionality Reduction | Blind Source Separation | #Components | Number of Modes |
|---|---|---|---|
| PCA | CP | 22 | 3 |
| | ICA | 28 | 0 |
| | SOBI | 16 | 3 |
| | SOBIRO | 14 | 3 |
| | ERICA | 16 | 3 |
| | AMUSE | 26 | 2 |
| NNMF | CP | 26 | 3 |
| | ICA | 28 | 0 |
| | SOBI | 32 | 2 |
| | SOBIRO | 22 | 3 |
| | ERICA | 28 | 0 |
| | AMUSE | 28 | 0 |

Table 3 – Summary of the results of the vibration response from the bench-scale building structure.

There could be several reasons why combining NNMF and ICA did not work for modal analysis:

- Incompatibility of assumptions: NNMF assumes that the data matrix is non-negative and can be factorized into a product of non-negative basis and coefficient matrices. ICA, on the other hand, assumes that the data is generated by statistically independent sources. The different assumptions made by the two techniques may not be compatible with each other, and the combined method may not be able to accurately capture the underlying structure of the data [88].

- Redundancy of information: NNMF and ICA are both techniques used for dimensionality reduction and feature extraction. Combining the two techniques may lead to redundancy of information and loss of important features.

- Choice of parameters: The performance of NNMF and ICA is highly dependent on the choice of parameters such as the number of components, regularization parameters, and initialization methods. The combined method may not have been properly optimized for the specific dataset and modal analysis problem.

AMUSE did not perfomed modal analysis in any level of this work. A possible explanation is that the method uses second-order statistics by constructing auto and cross-covariance matrices and simultaneously diagonalize these matrices to estimate the underlying mixing matrix. If the cross-covariance matrix is not symmetric, not only the extracted mixing matrices are sometimes complex but also the desired simultaneous diagonalization of matrix pair by a single matrix is not possible.

There is also a possibility of overfitting, i.e, the combination of PCA or NNMF and BSS algorithm may have overfitted the data, resulting in the identification of spurious modes that do not represent the underlying physics of the system.

SOBI and ERICA combined to NNMF, while worked for modal analysis applied to the cantilever beam structure video, did not work for the second scenario. In the first case NNMF algorithm can extract the underlying components that contribute to the overall motion of the system. The complexity of the system may cause the NNMF algorithm to be less effective. Also, the ERICA method is based on cumulants, which can be more challenging to accurately extract the dynamics characteristics from videos with complex motion.

In summary, the effectiveness of combining NNMF and a BSS method for modal analysis depends on the complexity of the system being analyzed. While this approach may work well for videos few degrees of freedom and monoarticulated structures, it may not be as effective for more complex systems.

# 5 Conclusions and Future Work

## 5.1 Conclusions

Several vision-based methods have successfully demonstrated reliability in performing structural dynamics identification, with the advantage of performing non-contact measurements. This work experimentally compared the performance of twelve different methods to extract three different modes from videos of an aluminum cantilever beam and a three-story building structure.

As these methods require BSS techniques, six different BSS solutions were investigated to analyze their applicability to perform modal estimation. From the results, the choice of the dimensionality reduction techniques plays an important role in the BSS algorithms performance. Overall, both PCA and NNMF are able to perform DR for full-field high-resolution structural dynamics analys from video.

For the cantilever beam structure, PCA-SOBI, PCA-AMUSE, NNMF-ICA and NNMF-AMUSE are suboptimal to idenfy all the three modes properly. The other eight methods proposed performed modal analysis accurately. It means that besisdes PCA-CP and NNMF-CP (already addressed in the literature to solve this specific problem), PCA-ICA, PCA-SOBIRO, PCA-ERICA, NNMF-SOBIRO, NNMF-SOBI and NNMF-ERICA are also good alternatives to structural dynamics analysis.

To find the modal coordinates and mode shapes of the three-story building structure, PCA-CP, PCA-SOBI, PCA-SOBIRO, PCA-ERICA, NNMF-CP and NNMF-SOBIRO are indicated. All of them were able to correctly identify the three natural frequencies concerning this structure. PCA-CP, PCA-SOBIRO, PCA-ERICA, NNMF-CP and NNMF-SOBIRO are the methods that strongly performed the modal analysis for both structures.

The combination of nonnegative matrix factorization and independent component analysis for modal analysis may fail due to different reasons.. Firstly, NNMF and ICA make different assumptions about the data, which may not be compatible with each other. Secondly, combining both techniques can lead to redundancy of information and loss of important features related to the modal analysis. Lastly, the performance of both techniques is dependent on various parameters, which may not have been optimized for the specific dataset and modal analysis problem.

It is relevant to analyse the NNMF-ERICA case. Here it is important to point out the sucess of this technique for the scenario using the cantilever beam structure and the failure of this technique for the test using the bench-scale building. The result indicates that the complexity of the system is a sensitive variable for this technique. In fact, the proposed methods which are based on PCA, are

found to be more robust from the point of view of increasing degrees of freedom.

Overall, the complexity of the system being analyzed plays a significant role, where NNMF may be less effective for systems with small displacements. Combining NNMF and a BSS method for modal analysis depends on the complexity of the system being analyzed. While it may work well for videos with limited movement, it may not be as effective for more complex systems.

In summary, methods based on dimensionality reduction and blind source separation algorithms are suitable and efective for modal identification. However, it is interesting to consider that their effectiveness depends on the complexity of the system being analyzed, as well as factors such as incompatible assumptions and the choice of parameters.

The results contribute to the video-based structural dynamics field assisting the choice of the dimensionality reduction algorithms and providing a range of alternatives to the blind source separation-based approaches. This work also encourage the study about the BSS problems for full-field high-resolution structural dynamics analys from video which are not currently explored in the literature of this specifc field.

## 5.2   Future Work

The modal identification here is limited to EMA in two different structures. As a future work, it is possible to investigate the proiminent methods for other structures or for specific cases of acquired videos. Other limitation is the manual choice of the output components for PCA and NNMF. The ideal number of components to perform DR can be studied as an optimization problem. A heuristic would be a solution to determine a near-optimal number of components for each method.

The techniques proposed here are only capable of performing in-plane motion analyses, requiring alternatives for identifying modes that manifest themselves as out-of-plane motions. Further tests are required to deal with out-of-plane motion and real-world conditions, such as operational and environmental variability caused by regular operation in structures.

Besides conventional consumer-grade video cameras, the described framework for video-based modal analysis can also be extended to work on other modalities of imagers. For example, neuromorphic event-based cameras [89], single-photon cameras [90], and time-of-flight imagers. They can also be adapted to work in applications requiring stereo-vision [91].

Recently studies suggest to explore video-based modal analysis techniques for physics-accurate digital twins of civil and mechanical infrastructures on the basis of neural radiance fields [92, 93]. Another applicability is to perform the data-fusion of conventional frame-based cameras along with high-speed event-based neuromorphic imagers to create high-fidelity and high extremely high frame-rate videos.

# Bibliography

1   FARRAR, C. R.; WORDEN, K. *Structural Health Monitoring: A Machine Learning Perspective*. Hoboken NJ, United States: John Wiley & Sons, Inc., 2013.   Cited on page 1.

2   ZAHID, F.; ONG, Z.; KHOO, S. A review of operational modal analysis techniques for in-service modal identification. *Journal of Sound and Vibration*, v. 42, n. 398, 2020.   Cited on page 1.

3   HE, J.; FU, Z. *Modal Analysis*. Oxford, United Kingdom: Butterworth-Heinemann Elsevier, 2001.   Cited on page 1.

4   MUGNAINI, V.; FRAGONARA, L. Z.; CIVERA, M. A machine learning approach for automatic operational modal analysis. *Mechanical Systems and Signal Processing*, v. 170, p. 108813, 2022. ISSN 0888-3270.   Cited on page 1.

5   REYNDERS, E. System identification methods for (operational) modal analysis: review andcomparison. *Archives of Computational Methods in Engineering*, v. 19, n. 51-124, 2012.   Cited on page 1.

6   VOLKMAR, R. et al. Experimental and operational modal analysis: Automated system identification for safety-critical applications. *Mechanical Systems and Signal Processing*, v. 183, p. 109658, 2023. ISSN 0888-3270.   Cited on page 1.

7   FAN, W.; QIAO, P. Vibration-based damage identification methods: A review and comparative study. *Structural Health Monitoring*, v. 10, n. 83-11, 2011.   Cited on page 2.

8   YANG, Y. et al. Blind identification of full-field vibration modes from video measurements with phase-based video motion magnification. *Mechanical Systems and Signal Processing*, v. 85, p. 567–590, 2017.   Cited 5 times on pages 2, 4, 18, 19, and 25.

9   CHEN, J. et al. Modal identification of simple structures with high-speed video using motion magnification. *Journal of Sound and Vibration*, v. 345, n. 58-71, 2015.   Cited on page 2.

10   MARTINEZ, B. et al. Sparse and random sampling techniques for high-resolution, full-field, bss-based structural dynamics identification from video. *Sensors*, v. 345, n. 58-71, 2020.   Cited 2 times on pages 2 and 4.

11   YANG, Y.; NAGARAJAIAH, S. Blind modal identification of output-only structures in time-domain based on complexity pursuit. *Earthquake Engineering & Structural Dynamics*, v. 42, p. 1885–1905, 10 2013.   Cited 2 times on pages 2 and 14.

12   SILVA, M. et al. Nonnegative matrix factorization-based blind source separation for full-field and high-resolution modal identification from video. *Journal of Sound and Vibration*, v. 487, p. 115586, 2020. ISSN 0022-460X.   Cited 7 times on pages 2, 5, 11, 12, 13, 21, and 25.

13   YANG, Y.; FARRAR, C.; MASCARENAS, D. Full-field structural dynamics by video motion manipulations. In: SPRINGER. *International Digital Imaging Correlation Society: Proceedings of the First Annual Conference, 2016*. [S.l.], 2017. p. 223–226.   Cited 2 times on pages 2 and 21.

14   YANG, Y.; NAGARAJAIAH, S. Output-only modal identification with limited sensors using sparse component analysis. *Journal of Sound and Vibration*, v. 332, n. 19, p. 4741–4765, 2013. ISSN 0022-460X.   Cited on page 2.

15   LIU, T. et al. A comparative study of four kinds of adaptive decomposition algorithms and their applications. *Sensors*, MDPI, v. 18, n. 7, p. 2120, 2018.   Cited on page 2.

16   PAL, M. et al. Blind source separation: A review and analysis. In: IEEE. *2013 International Conference Oriental COCOSDA held jointly with 2013 Conference on Asian Spoken Language Research and Evaluation*. [S.l.], 2013. p. 1–5.   Cited on page 2.

17   YANG, Z. et al. Blind source separation by nonnegative matrix factorization with minimum-volume constraint. In: *2010 International Conference on Intelligent Control and Information Processing*. [S.l.: s.n.], 2010. p. 117–119.   Cited on page 2.

18   SADHU, A.; NARASIMHAN, S.; ANTONI, J. A review of output-only structural mode identification literature employing blind source separation methods. *Mechanical Systems and Signal Processing*, v. 94, p. 415–431, 2017. ISSN 0888-3270.   Cited 2 times on pages 2 and 13.

19   WANG, Y. X.; ZHANG, Y. J.  Nonnegative Matrix Factorization: A Comprehensive Review. *IEEE Transactions on Knowledge and Data Engineering*, v. 25, n. 6, 2013.   Cited on page 2.

20   CICHOCKI, A.; ZDUNEK, R.; AMARI, S. New algorithms for non-negative matrix factorization in applications to blind source separation. In: *2006 IEEE International Conference on Acoustics Speech and Signal Processing Proceedings*. [S.l.: s.n.], 2006. v. 5.   Cited on page 2.

21   MUSAFERE, F.; SADHU, A.; LIU, K. Towards damage detection using blind source separation integrated with time-varying auto-regressive modeling. *Smart Materials and Structures*, IOP Publishing, v. 25, n. 1, p. 015013, nov 2015.   Cited on page 2.

22   CHENG, L.; TONG, F. Application of blind source separation algorithms and ambient vibration testing to the health monitoring of concrete dams. *Mathematical Problems in Engineering*, Hindawi, v. 2016, 2016.   Cited 2 times on pages 3 and 13.

23   PONCELET, F. et al. Output-only modal analysis using blind source separation techniques. *Mechanical Systems and Signal Processing*, v. 21, n. 6, p. 2335–2358, 2007. ISSN 0888-3270.   Cited on page 3.

24   LI, X. et al. A frequency domain blind identification method for operational modal analysis using a limited number of sensors. *Journal of Vibration and Control*, v. 26, n. 1383-1398, 2016.   Cited 3 times on pages 3, 13, and 21.

25   ZHOU, W.; CHELIDZE, D. Blind source separation based vibration mode identification. *Mechanical systems and signal processing*, Elsevier, v. 21, n. 8, p. 3072–3087, 2007.   Cited 3 times on pages 3, 15, and 21.

26   WANG, J. et al. Comparison of different independent component analysis algorithms for output-only modal analysis. *Shock and Vibration*, Hindawi, v. 2016, 2016.   Cited 2 times on pages 3 and 21.

27   SHANNO, D. F. Conditioning of quasi-newton methods for function minimization. *Mathematics of computation*, v. 24, n. 111, p. 647–656, 1970.   Cited on page 3.

28   AKUZAWA, T. Extended quasi-newton method for the ica. In: *Proceedings of the International Workshop on Independent Component Analysis and Blind Signal Separation*. [S.l.: s.n.], 2000. p. 521–525.   Cited 2 times on pages 3 and 16.

29   ANTONI, J.; CHAUHAN, S. A study and extension of second-order blind source separation to operational modal analysis. *Journal of Sound and Vibration*, Elsevier, v. 332, n. 4, p. 1079–1106, 2013.   Cited 2 times on pages 3 and 21.

30   ANTONI, J.; CASTIGLIONE, R.; GARIBALDI, L. Interpretation and generalization of complexity pursuit for the blind separation of modal contributions. *Mechanical Systems and Signal Processing*, Elsevier, v. 85, p. 773–788, 2017.   Cited 2 times on pages 3 and 21.

31   SILVA, M.; GREEN, A.; MASCAREÑAS, D. A generalized technique for full-field blind identification of travelling waves and complex modes from video measurements with hilbert transform. In: SPRINGER. *Data Science in Engineering, Volume 9: Proceedings of the 39th IMAC, A Conference and Exposition on Structural Dynamics 2021*. [S.l.], 2022. p. 233–236.   Cited 3 times on pages 5, 19, and 21.

32   AYESHA, S.; HANIF, M. K.; TALIB, R. Overview and comparative study of dimensionality reduction techniques for high dimensional data. *Information Fusion*, v. 59, p. 44–58, 2020. ISSN 1566-2535.   Cited on page 8.

33   MAATEN, L. V. D. et al. Dimensionality reduction: a comparative review. *J Mach Learn Res*, v. 10, n. 66-71, p. 13, 2009.   Cited 2 times on pages 8 and 9.

34   PEARSON, K. On lines and planes of closest fit to systems of points in space. *The London, Edinburgh, and Dublin philosophical magazine and journal of science*, Taylor & Francis, v. 2, n. 11, p. 559–572, 1901.   Cited on page 9.

35   HOTELLING, H. Analysis of a complex of statistical variables into principal components. *Journal of educational psychology*, Warwick & York, v. 24, n. 6, p. 417, 1933.   Cited on page 9.

36   DEEGALLA, S.; BOSTRÖM, H.; WALGAMA, K. Choice of dimensionality reduction methods for feature and classifier fusion with nearest neighbor classifiers. In: IEEE. *2012 15th International Conference on Information Fusion*. [S.l.], 2012. p. 875–881.   Cited on page 9.

37   KURITA, T. Principal component analysis (pca). *Computer Vision: A Reference Guide*, Springer, p. 1–4, 2019.   Cited on page 9.

38   JOLLIFFE, I. T.; CADIMA, J. Principal component analysis: a review and recent developments. *Philosophical transactions of the royal society A: Mathematical, Physical and Engineering Sciences*, The Royal Society Publishing, v. 374, n. 2065, p. 20150202, 2016.   Cited on page 9.

39   THARWAT, A. Principal component analysis-a tutorial. *International Journal of Applied Pattern Recognition*, Inderscience Publishers (IEL), v. 3, n. 3, p. 197–240, 2016.   Cited on page 9.

40   ZHAO, H. et al. Fault diagnosis method based on principal component analysis and broad learning system. *IEEE Access*, IEEE, v. 7, p. 99263–99272, 2019.   Cited on page 9.

41   GILLIS, N. The why and how of nonnegative matrix factorization. *Connections*, v. 12, n. 2, 2014.   Cited on page 11.

42   LEE, D. D.; SEUNG, H. S. Learning the parts of objects by non-negative matrix factorization. *Nature*, Nature Publishing Group UK London, v. 401, n. 6755, p. 788–791, 1999.   Cited 2 times on pages 11 and 12.

43   GUILLAMET, D.; VITRIA, J. Non-negative matrix factorization for face recognition. In: SPRINGER. *Topics in Artificial Intelligence: 5th Catalonian Conference on AI, CCIA 2002 Castellón, Spain, October 24–25, 2002 Proceedings*. [S.l.], 2002. p. 336–344.   Cited on page 11.

44   LUO, X. et al. Symmetric nonnegative matrix factorization-based community detection models and their convergence analysis. *IEEE Transactions on Neural Networks and Learning Systems*, IEEE, v. 33, n. 3, p. 1203–1215, 2021.   Cited on page 11.

45   KRIEBEL, A. R.; WELCH, J. D. Uinmf performs mosaic integration of single-cell multi-omic datasets using nonnegative matrix factorization. *Nature communications*, Nature Publishing Group UK London, v. 13, n. 1, p. 780, 2022.   Cited on page 11.

46   SU, X. et al. A deep learning method for repurposing antiviral drugs against new viruses via multi-view nonnegative matrix factorization and its application to sars-cov-2. *Briefings in bioinformatics*, Oxford University Press, v. 23, n. 1, p. bbab526, 2022.   Cited on page 11.

47   PAATERO, P.; TAPPER, U. Positive matrix factorization: A non-negative factor model with optimal utilization of error estimates of data values. *Environmetrics*, Wiley Online Library, v. 5, n. 2, p. 111–126, 1994.   Cited on page 12.

48   LIN, C.-J. Projected gradient methods for nonnegative matrix factorization. *Neural computation*, MIT Press, v. 19, n. 10, p. 2756–2779, 2007.   Cited on page 12.

49   BERRY, M. W. et al. Algorithms and applications for approximate nonnegative matrix factorization. *Computational statistics & data analysis*, Elsevier, v. 52, n. 1, p. 155–173, 2007.   Cited on page 12.

50   HERAULT, J.; JUTTEN, C. Space or time adaptive signal processing by neural network models. In: AMERICAN INSTITUTE OF PHYSICS. *AIP conference proceedings*. [S.l.], 1986. v. 151, n. 1, p. 206–211.   Cited on page 12.

51   YU, X.; HU, D.; XU, J. *Blind source separation: theory and applications*. [S.l.]: John Wiley & Sons, 2013.   Cited on page 13.

52   LIU, C.; ZHANG, C. Remove artifacts from a single-channel eeg based on vmd and sobi. *Sensors*, MDPI, v. 22, n. 17, p. 6698, 2022.   Cited on page 13.

53   BRIDWELL, D. A. et al. Spatiospectral decomposition of multi-subject eeg: evaluating blind source separation algorithms on real and realistic simulated data. *Brain topography*, Springer, v. 31, p. 47–61, 2018.   Cited on page 13.

54   VINCENT, E. et al. From blind to guided audio source separation: How models and side information can improve the separation of sound. *IEEE Signal Processing Magazine*, IEEE, v. 31, n. 3, p. 107–115, 2014.   Cited on page 13.

55   GANNOT, S. et al. A consolidated perspective on multimicrophone speech enhancement and source separation. *IEEE/ACM Transactions on Audio, Speech, and Language Processing*, IEEE, v. 25, n. 4, p. 692–730, 2017.   Cited on page 13.

56   GHOSH, B. et al. Automatic detection of volcanic unrest using blind source separation with a minimum spanning tree based stability analysis. *IEEE Journal of Selected Topics in Applied Earth Observations and Remote Sensing*, IEEE, v. 14, p. 7771–7787, 2021.   Cited on page 13.

57   MESCHEDE, M.; STUTZMANN, E.; SCHIMMEL, M. Blind source separation of temporally independent microseisms. *Geophysical Journal International*, Oxford University Press, v. 216, n. 2, p. 1260–1275, 2019.   Cited on page 13.

58   SWAMINATHAN, B.; SHARMA, B.; CHAUHAN, S. Utilization of blind source separation techniques for modal analysis. In: SPRINGER. *Structural Dynamics, Volume 3: Proceedings of the 28th IMAC, A Conference on Structural Dynamics, 2010*. [S.l.], 2011. p. 189–206.   Cited on page 13.

59   SADHU, A. Blind source separation: a generalized modal identification tool for civil structures. In: SPRINGER. *Dynamics of Civil Structures, Volume 2: Proceedings of the 33rd IMAC, A Conference and Exposition on Structural Dynamics, 2015*. [S.l.], 2015. p. 39–47.   Cited on page 13.

60   CHOI, S. et al. Blind source separation and independent component analysis: A review. *Neural Information Processing-Letters and Reviews*, v. 6, n. 1, p. 1–57, 2005.   Cited on page 13.

61   ULLAH, Z. et al. Time-domain output data identification model for pipeline flaw detection using blind source separation technique complexity pursuit. In: MDPI. *Acoustics*. [S.l.], 2019. v. 1, n. 1, p. 199–219.   Cited on page 13.

62   JALALI, S.; MALEKI, A. Minimum complexity pursuit. In: IEEE. *2011 49th Annual Allerton Conference on Communication, Control, and Computing (Allerton)*. [S.l.], 2011. p. 1764–1770.   Cited on page 14.

63   STONE, J. Blind source separation using temporal predictability. *Neural computation*, v. 13, p. 1559–74, 08 2001.   Cited on page 14.

64   HYVÄRINEN, A. Complexity pursuit: separating interesting components from time series. *Neural computation*, MIT Press One Rogers Street, Cambridge, MA 02142-1209, USA, v. 13, n. 4, p. 883–898, 2001.   Cited on page 14.

65   SHI, Z.; JIANG, Z.; YIN, J. Generalized complexity pursuit. In: *2008 Fourth International Conference on Natural Computation*. [S.l.: s.n.], 2008. v. 3, p. 199–203.   Cited on page 14.

66   STONE, J. V. Independent component analysis: an introduction. *Trends in cognitive sciences*, Elsevier, v. 6, n. 2, p. 59–64, 2002.   Cited on page 14.

67   HYVÄRINEN, A. Independent component analysis: recent advances. *Philosophical Transactions of the Royal Society A: Mathematical, Physical and Engineering Sciences*, The Royal Society Publishing, v. 371, n. 1984, p. 534, 2013.   Cited on page 14.

68   JUAN, E. S. et al. Proposed integration algorithm to optimize the separation of audio signals using the ica and wavelet transform. In: SPRINGER. *Image and Signal Processing: 9th International Conference, ICISP 2020, Marrakesh, Morocco, June 4–6, 2020, Proceedings 9*. [S.l.], 2020. p. 367–376. Cited on page 14.

69   GOPINATH, K. S. et al. Exploring brain mechanisms underlying gulf war illness with group ica based analysis of fmri resting state networks. *Neuroscience letters*, Elsevier, v. 701, p. 136–141, 2019. Cited on page 14.

70  BELOUCHRANI, A. et al. A blind source separation technique using second-order statistics. *IEEE Transactions on signal processing*, IEEE, v. 45, n. 2, p. 434–444, 1997. Cited on page 15.

71  OLIVEIRA, D. R. de et al. Second order blind identification algorithm with exact model order estimation for harmonic and interharmonic decomposition with reduced complexity. *International Journal of Electrical Power & Energy Systems*, Elsevier, v. 125, p. 106415, 2021. Cited on page 15.

72  BELOUCHRANI, A. et al. Second-order blind separation of temporally correlated sources. In: CITESEER. *Proc. Int. Conf. Digital Signal Processing*. [S.l.], 1993. p. 346–351. Cited on page 15.

73  BRAGA, E. de Q.; TIERRA-CRIOLLO, C. J.; MANZANO, G. M. Sobi with robust orthogonalization to remove the artefact stimulus in evoked potential-5hz current sinusoidal stimulus. In: SCITEPRESS. *International Conference on Bio-inspired Systems and Signal Processing*. [S.l.], 2008. v. 2, p. 273–276. Cited on page 15.

74  CHOI, S.; CICHOCKI, A.; BELOUCHARNI, A. Second order nonstationary source separation. *Journal of VLSI signal processing systems for signal, image and video technology*, Springer, v. 32, p. 93–104, 2002. Cited on page 15.

75  CRUCES, S.; CASTEDO, L.; CICHOCKI, A. Novel blind source separation algorithms using cumulants. In: IEEE. *2000 IEEE International Conference on Acoustics, Speech, and Signal Processing. Proceedings*. [S.l.], 2000. v. 5, p. 3152–3155. Cited on page 16.

76  BRIGHAM, K.; KUMAR, B. V. Imagined speech classification with eeg signals for silent communication: a preliminary investigation into synthetic telepathy. In: IEEE. *2010 4th International Conference on Bioinformatics and Biomedical Engineering*. [S.l.], 2010. p. 1–4. Cited on page 16.

77  TONG, L. et al. Amuse: a new blind identification algorithm. In: IEEE. *IEEE international symposium on circuits and systems*. [S.l.], 1990. p. 1784–1787. Cited on page 16.

78  MIETTINEN, J. et al. Statistical properties of a blind source separation estimator for stationary time series. *Statistics & Probability Letters*, Elsevier, v. 82, n. 11, p. 1865–1873, 2012. Cited on page 16.

79  TONG, L. et al. Indeterminacy and identifiability of blind identification. *IEEE Transactions on circuits and systems*, IEEE, v. 38, n. 5, p. 499–509, 1991. Cited on page 16.

80  FELDMAN, M. Hilbert transform in vibration analysis. *Mechanical systems and signal processing*, Elsevier, v. 25, n. 3, p. 735–802, 2011. Cited on page 18.

81  KSCHISCHANG, F. R. The hilbert transform. *University of Toronto*, Citeseer, v. 83, p. 277, 2006. Cited on page 18.

82  MCNEILL, S.; ZIMMERMAN, D. A framework for blind modal identification using joint approximate diagonalization. *Mechanical Systems and Signal Processing*, v. 22, n. 7, p. 1526 – 1548, 2008. ISSN 0888-3270. Cited on page 19.

83  CHEN, J. G. et al. Developments with motion magnification for structural modal identification through camera video. In: SPRINGER. *Dynamics of Civil Structures, Volume 2: Proceedings of the 33rd IMAC, A Conference and Exposition on Structural Dynamics, 2015*. [S.l.], 2015. p. 49–57. Cited on page 19.

84  ALLADA, V.; SARAVANAN, T. J. Computer vision technique for blind identification of modal frequency of structures from video measurements. *Engineering Proceedings*, Multidisciplinary Digital Publishing Institute, v. 10, n. 1, p. 12, 2021. Cited on page 19.

85  PASTOR, M.; BINDA, M.; HARČARIK, T. Modal assurance criterion. *Procedia Engineering*, Elsevier, v. 48, p. 543–548, 2012.  Cited 2 times on pages 22 and 23.

86  ALLEMANG, R. J. The modal assurance criterion–twenty years of use and abuse. *Sound and vibration*, v. 37, n. 8, p. 14–23, 2003.  Cited on page 22.

87  TING, T.; CHEN, T.; TWOMEY, W. Correlating mode shapes based on the modal assurance criterion. *Finite Elements in Analysis and Design*, Elsevier, v. 14, n. 4, p. 353–360, 1993.  Cited on page 22.

88  ZHANG, J. et al. Pattern expression nonnegative matrix factorization: algorithm and applications to blind source separation. *Computational intelligence and neuroscience*, Hindawi, v. 2008, 2008.  Cited on page 40.

89  GOTHARD, A. et al. Digital coded exposure formation of frames from event-based imagery. *Neuromorphic Computing and Engineering*, IOP Publishing, v. 2, n. 1, p. 014005, 2022.  Cited on page 42.

90  SHIN, D. et al. Photon-efficient imaging with a single-photon camera. *Nature communications*, Nature Publishing Group UK London, v. 7, n. 1, p. 12046, 2016.  Cited on page 42.

91  NAM, Y. et al. Stereo depth from events cameras: Concentrate and focus on the future. In: *Proceedings of the IEEE/CVF Conference on Computer Vision and Pattern Recognition*. [S.l.: s.n.], 2022. p. 6114–6123.  Cited on page 42.

92  MILDENHALL, B. et al. Nerf: Representing scenes as neural radiance fields for view synthesis. *Communications of the ACM*, ACM New York, NY, USA, v. 65, n. 1, p. 99–106, 2021.  Cited on page 42.

93  DAVIS, A. et al. Digital twins for photorealistic event-based structural dynamics. In: . [S.l.: s.n.], 2023.  Cited on page 42.